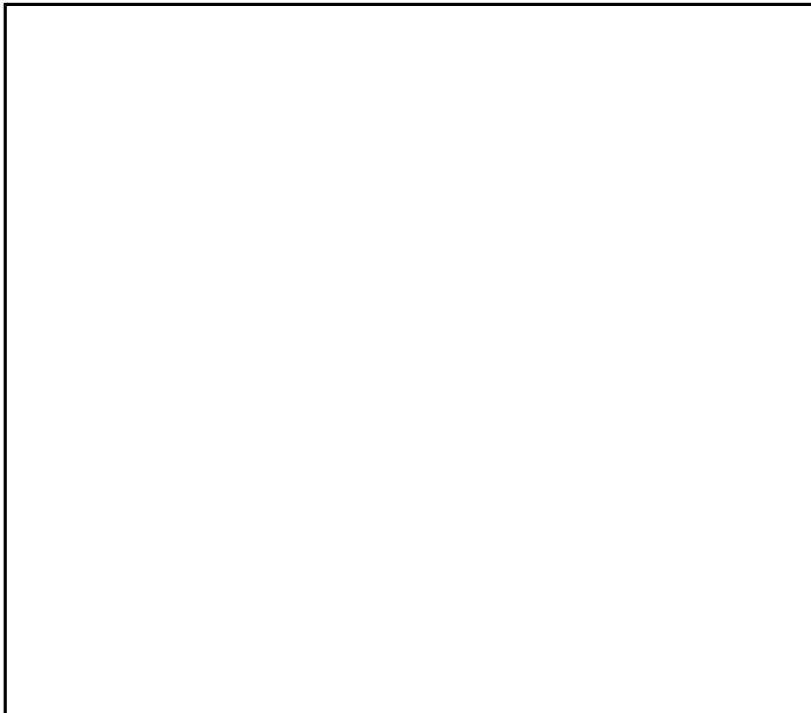


DECLASS REVIEW by NIMA/DOD

STATINTL



#1

REPORT

STAT

HYDROMATIC LIQUID BEARING
ASSESSMENT

RM-135-65
June 1965

STATINTL

[Redacted]

STAT

FOREWORD

STATINTL

[Redacted]

submits this report in compliance with Item 3.1

of the Development Objectives of

[Redacted]

STAT

STATINTL

[Redacted]


Research Manager

Approved:



STAT

ABSTRACT

Two approaches to the improvement of liquid bearings are feasible: the first is to improve the efficiency of the bearing to require lower horse-power input from a centrifugal pump, the second is to conceive a design in which an external pump and plumbing are eliminated by integrating a pump within the bearing itself (Assignment 

STAT

This assignment was issued to experimentally assess the state-of-the-art in liquid bearing research, design, and development and, if possible, improve existing concepts in preparation for a new generation of photographic processors. Such factors as efficiency, economy, simplicity, self-centering, elimination of guide flanges, and no necessity for format changes to accommodate different film widths were to be considered. To be given special attention were the advantages, if any, of slots over hole jets as a film cushion support.

SUMMARY

This final report compiles data obtained on an exhaustive series of tests on narrow liquid bearing prototype designs of single-slot, end-feed bearings of varying cross section and material of construction, as well as center-feed, self-centering bearings and end-feed tapered-slot self-centering bearings. Certain hydrodynamic relationships were established and a new concept of bearing design was evolved. To duplicate the "crown effect" of belt roller, self-adjusting tracking, a reverse crown, or "bow tie" pressure profile is necessary for hydraulic bearings. A bearing was designed, constructed, and tested which exhibited self-aligning features, imparted rotary motion to the film, and promised to be self-adjusting to changing load conditions at constant flow. While it appeared not to require guide flanges for operational stability, it did require format changes for different film widths. Thus, not all of the design objectives were achieved, but the advantages and shortcomings of the final design are discussed in detail.

CONTENTS

SECTION		PAGE
1	INTRODUCTION	1-1
	1.1 BEARING CONCEPT	1-1
	1.2 PURPOSE AND OBJECTIVES	1-2
2	TECHNICAL DISCUSSION	2-1
	2.1 EQUIPMENT AND INSTRUMENTATION	2-1
	2.2 BEARING EXPERIMENTATION	2-1
	2.2.1 Narrow Liquid Bearing Prototype	2-1
	2.2.2 Liquid Bearing Slot Data	2-14
	2.2.3 Self-Centering Liquid Bearings	2-27
	2.2.4 Methacrylate End-Feed Self-Centering Liquid Bearing	2-34
3	SUMMATION OF FINDINGS	3-1
	3.1 NARROW LIQUID BEARINGS	3-1
	3.2 END-FEED LIQUID BEARINGS	3-1
	3.3 SELF-CENTERING LIQUID BEARINGS	3-2
	3.3.1 Liquid Bearing Design Procedure	3-2
	BIBLIOGRAPHY	3-7
	.APPENDIX	
A	EQUIPMENT AND INSTRUMENTATION	A-1
B	PRESSURE GRADIENT CHARACTERISTICS	B-1

ILLUSTRATIONS

FIGURE		PAGE
2-1	Liquid Bearing Test Rack	2-2
2-2	Rotameter Calibration Chart	2-3
2-3	Friction Factors for Straight, Clean, Round Pipes	2-4
2-4	Vernier Depth Gage	2-5
2-5	Narrow Prototype Liquid Bearing	2-6
2-6	Narrow Prototype Liquid Bearing Pressure Profile (0.067" Slot)	2-7
2-7	Analysis of Pressure-Flow Relationship	2-11
2-8	Narrow Prototype Liquid Bearing with Cerrobend Plenum and Plastic Wedge	2-13
2-9	Narrow Prototype Liquid Bearing with Wide Slot	2-15
2-10	Five Stainless-Steel Bearings - All Slots 0.063 x 9-1/2 Inches	2-18
2-11	Pressure Profile for 1.000" I.D. Circular Stainless Bearing	2-19
2-12	Pressure Profile for 1.250" I.D. Circular Stainless Bearing	2-20
2-13	Pressure Profile for 1.500" I.D. Circular Stainless Bearing	2-21
2-14	Pressure Profile for 1.620" I.D. Circular Stainless Bearing	2-22
2-15	Pressure Profile for 1.875" I.D. Circular Stainless Bearing	2-23
2-16	Pressure vs. Flow for Experimental Bearings	2-24
2-17	Pressure Profile for 1.500" I.D. Circular Copper Bearing	2-28
2-18	Double-Plenum Center-Feed Copper Bearing	2-31
2-19	Pressure Profile of Center-Feed Copper Bearing	2-32

ILLUSTRATIONS (Continued)

FIGURE		PAGE
2-20	Logarithmic Slot Self-Centering Liquid Bearing	2-33
2-21	Methacrylate Self-Centering Bearing	2-35
2-22	Cutaway Showing Construction of Methacrylate Tapered-Slot, Self-Centering Bearing	2-36
2-23	Annular Velocity Versus Supported Weight - 9-1/2-Inch Film	2-40
2-24	Cushion Height at Constant Flow and Varying Weight - 9-1/2-Inch Film	2-41
2-25	Annular and Transverse Areas at Different Weight Loadings - 9-1/2-Inch Film	2-42
2-26	Pressure Profile for Tapered-Slot Liquid Bearing 9-1/2-Inch Width	2-45
2-27	Annular Velocity Versus Supported Weight - 6.6-Inch Film	2-49
2-28	Cushion Height at Constant Flow and Varying Weight - 6.6-Inch Film	2-50
2-29	Annular and Transverse Areas at Different Weight Loadings - 6.6-Inch Film	2-51
2-30	Pressure Profile for Tapered-Slot Bearing 6.6-Inch Width	2-52

TABLES

TABLE		PAGE
2-1	FLOWMETER CALIBRATION DATA AND REYNOLDS NUMBER CALCULATION	2-8
2-2	PRESSURE PROFILE MEASUREMENT DATA FOR NARROW PROTOTYPE LIQUID BEARINGS	2-9
2-3	WITH CERROBEND AND METHACRYLATE WEDGE IN PLENUM	2-9
2-4	PRESSURE PROFILE MEASUREMENT DATA FOR NARROW PROTOTYPE LIQUID BEARINGS	2-16
2-5	PRESSURE PROFILE MEASUREMENT DATA FOR NARROW PROTOTYPE LIQUID BEARINGS	2-16
2-6	PRESSURE PROFILE MEASUREMENT DATA FOR CIRCULAR CROSS-SECTION LIQUID BEARING	2-25
2-7	PRESSURE PROFILE MEASUREMENT DATA FOR CIRCULAR CROSS-SECTION LIQUID BEARING	2-25
2-8	PRESSURE PROFILE MEASUREMENT DATA FOR CIRCULAR CROSS-SECTION LIQUID BEARING	2-26
2-9	PRESSURE PROFILE MEASUREMENT DATA FOR CIRCULAR CROSS-SECTION LIQUID BEARING	2-26
2-10	PRESSURE PROFILE MEASUREMENT DATA FOR CIRCULAR CROSS-SECTION LIQUID BEARING	2-29
2-11	PRESSURE PROFILE MEASUREMENT DATA FOR CIRCULAR CROSS-SECTION LIQUID BEARING	2-29
2-12	ANNULAR VELOCITY, CUSHION HEIGHT, SUPPORTED WEIGHT	2-39
2-13	PRESSURE PROFILE MEASUREMENT DATA FOR TAPERED-SLOT LIQUID BEARING	2-46
2-14	PRESSURE PROFILE MEASUREMENT DATA FOR TAPERED-SLOT LIQUID BEARING	2-46
2-15	BEARING SLOT WIDTHS	2-47
2-16	ANNULAR VELOCITY, CUSHION HEIGHT, SUPPORTED WEIGHT	2-53

SECTION 1
INTRODUCTION

1.1 BEARING CONCEPT

Prior to the innovation of the air and liquid bearing concept, all commercial film processing units transported film on a series of rollers (similar to the setup of a paper mill) or sprocket gears that matched the perforations in standard types of perforated film. These conventional machines use a preponderance of driven rollers, each of which must be rotated at precisely the same speed as every other roller. If they are not, one of two problems develops.

The first problem occurs when a variation of speed in the pressure roller groups in either the wet or dry end of the processing line causes the formation of a slack loop. This slack allows the film to slap against parts of the processor or to cohere and damage itself by abrasion. The second occurs when the film is suddenly shortened, which produces stretching, ruffling, or even film breakage.

With sprocket gears instead of rollers, the film can lose tracking or its perforations can be torn. Any of these conditions, including the normal slippage over a smooth roller, results in film damage, intolerable in certain aerial surveillance and other irreplaceable original negative films.

The liquid and air bearing principle, conceived by [REDACTED] was a significant contribution to the state-of-the-art. Its development has advanced film processor design and has resulted in a new generation of equipment. By providing a fluid cushion on each bearing in the wet end of the machine and an air cushion in the drier section, the film could literally be floated through the complete processing cycle contacting only its drive

STAT

capstan and takeup spool. The supporting fluid cushion was created by ejecting jets of liquid from within a cylindrical plenum. These jets, by impinging on the film passing over the bearing, created a firm liquid layer in the annular space. The air bearing is similar in principle.

Thus, in theory, the only frictional forces to which the film is subjected, are the intermolecular drag coefficients and liquid viscosity factors at the boundary interfaces. In practice, however, it proved necessary to provide film guide flanges at either end to control the effluent. Although these flanges were placed far enough apart to allow for the width of film being used, there was still considerable edge friction due to erratic film tracking along its multiple-bearing pathway in the processor.

One of the serendipities of the design concept proved to be this: because the liquid creating the cushion in each stage of the processor (developer, stop bath, fixer, etc.) was the chemical solution itself, greater penetration of the emulsion was achieved, resulting in reduced time of contact.

1.2 PURPOSE AND OBJECTIVES

In view of the state-of-the-art briefly outlined in the preceding section, the objectives of this facet of the research program became clear. Improve mechanical efficiency and reduce horsepower requirements while increasing cushion stability. Eliminate guide flanges by designing a self-centering bearing. Develop a bearing that, in ideal configuration, would not require format changes to accommodate different widths of film. Establish design criteria so that bearing performance could be predicted before fabrication.

SECTION 2

TECHNICAL DISCUSSION

2.1 EQUIPMENT AND INSTRUMENTATION

The details of assembly and adjunctive mensuration devices for the liquid bearing test rack (Figure 2-1) are presented in Appendix A. One significant change was made in the test apparatus between the issuance of the February Interim Report and this final paper. The closed-circuit recirculatory system illustrated introduced cyclic time fluctuations because of the pump design and its proximity to the liquid bearing under test. Rather than designing and building a pulse-smoothing device for insertion in the line, the problem was largely eliminated by connecting the municipal water faucet outlet directly to the flowmeter inlet. This meant, of course, that the tank drain had to be opened during a test run to prevent overflow and that the possibility of tempering the water temperature was eliminated. However, the flow was greatly stabilized.

A new sensing pitot probe was built consisting of an 0.008-inch inside-diameter steel capillary tube mounted in a 1/4-inch thin-wall tube. The device was further improved by providing a tee at its outlet to prevent having to bleed air bubbles from the long plastic hose connecting it to the inclined manometer. This refinement greatly facilitated rapid measurement of static pressures in the three slots during testing.

2.2 BEARING EXPERIMENTATION

2.2.1 Narrow Liquid Bearing Prototype

The first series of experiments was performed on an experimental stainless-steel bearing (Figures 2-5, 2-6, and Table 2-2). Its overall length was 13.9 inches and the inside diameter of its throat was 1.0 inch.

(Continued page 2-10)

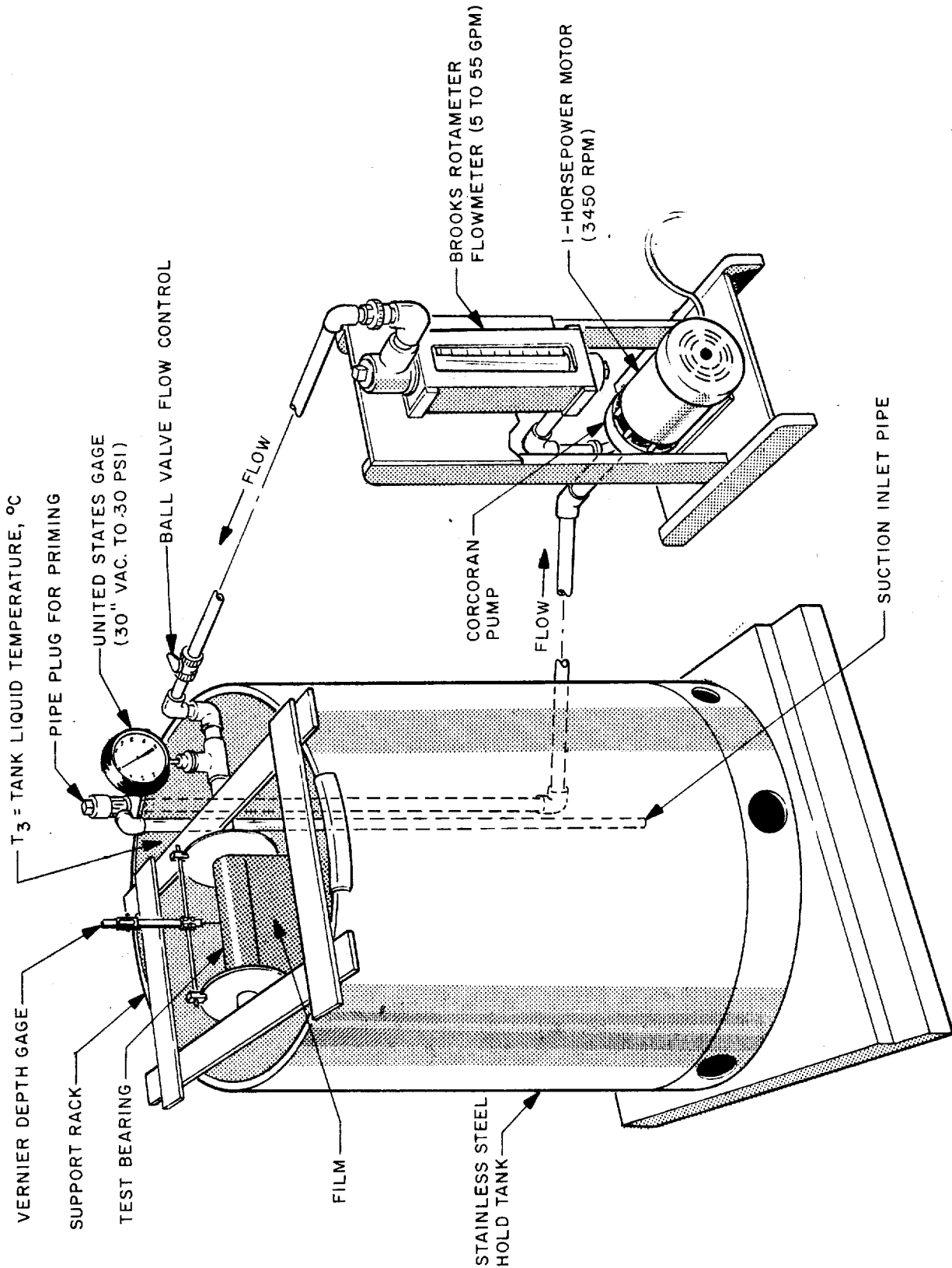
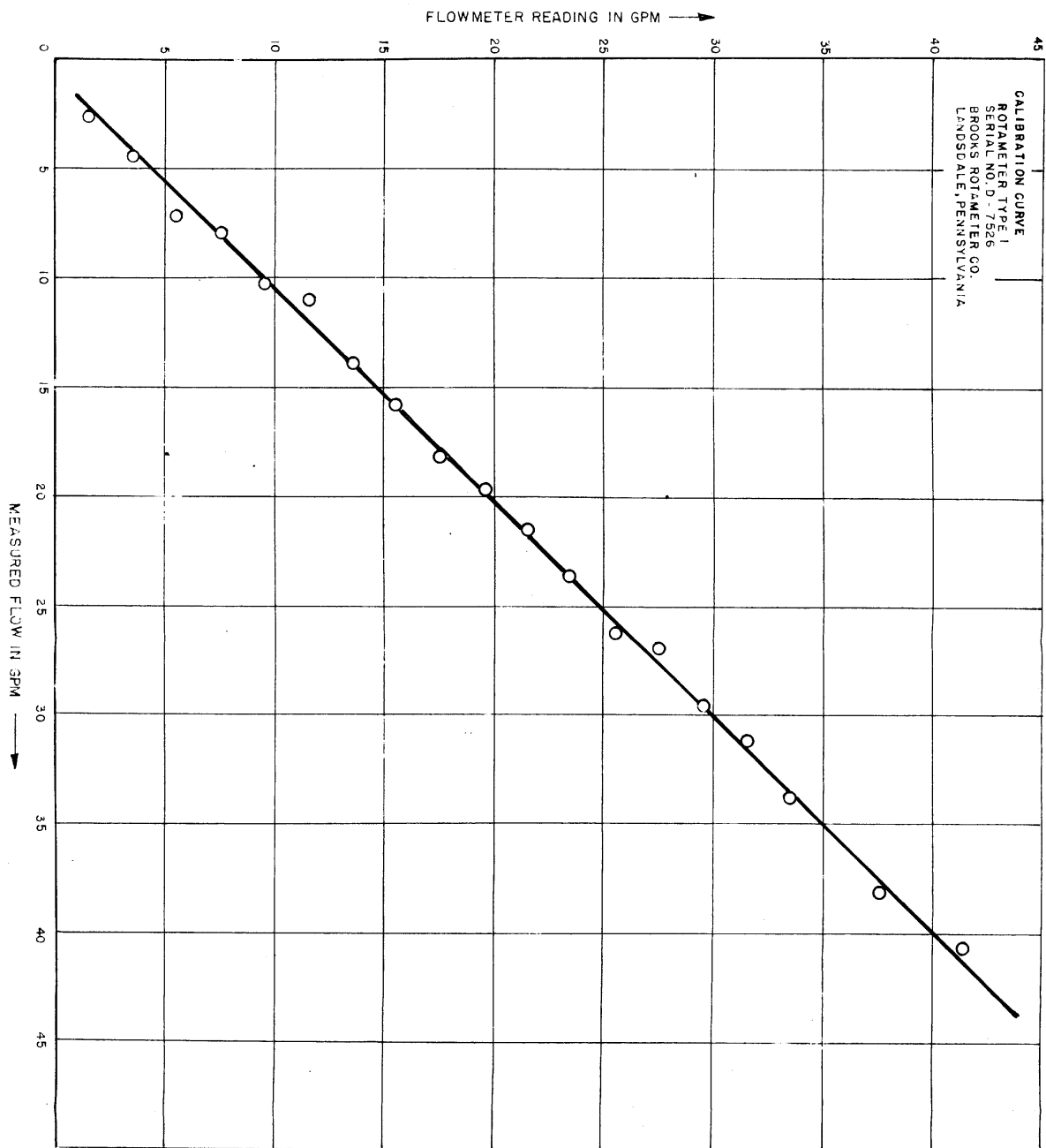


Figure 2-1. Liquid Bearing Test Rack

50073



STAT

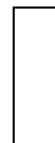


Figure 2-2. Rotameter Calibration Chart

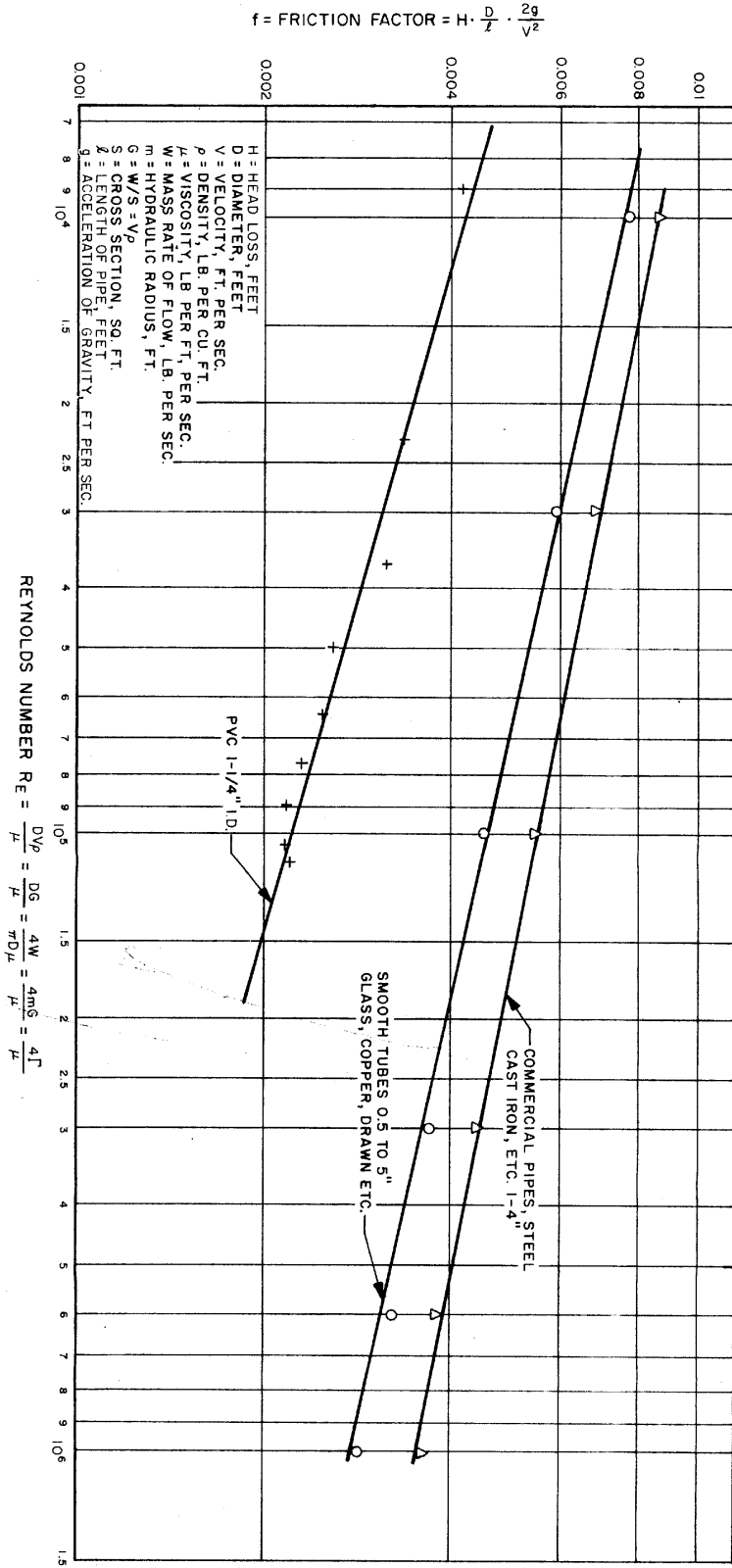


Figure 2-3. Friction Factors For Straight, Clean, Round Pipes

STAT

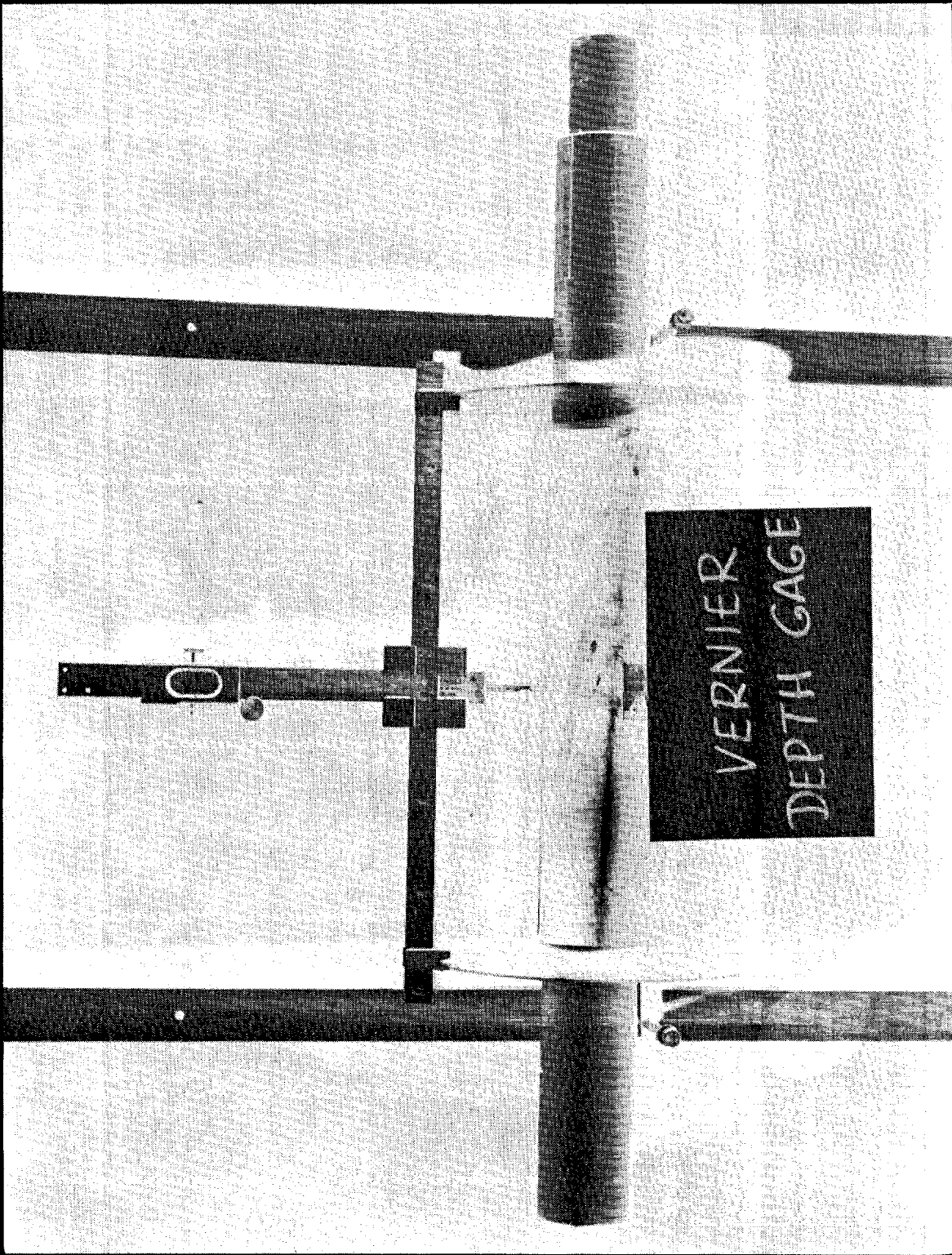


Figure 2-4. Vernier Depth Gage

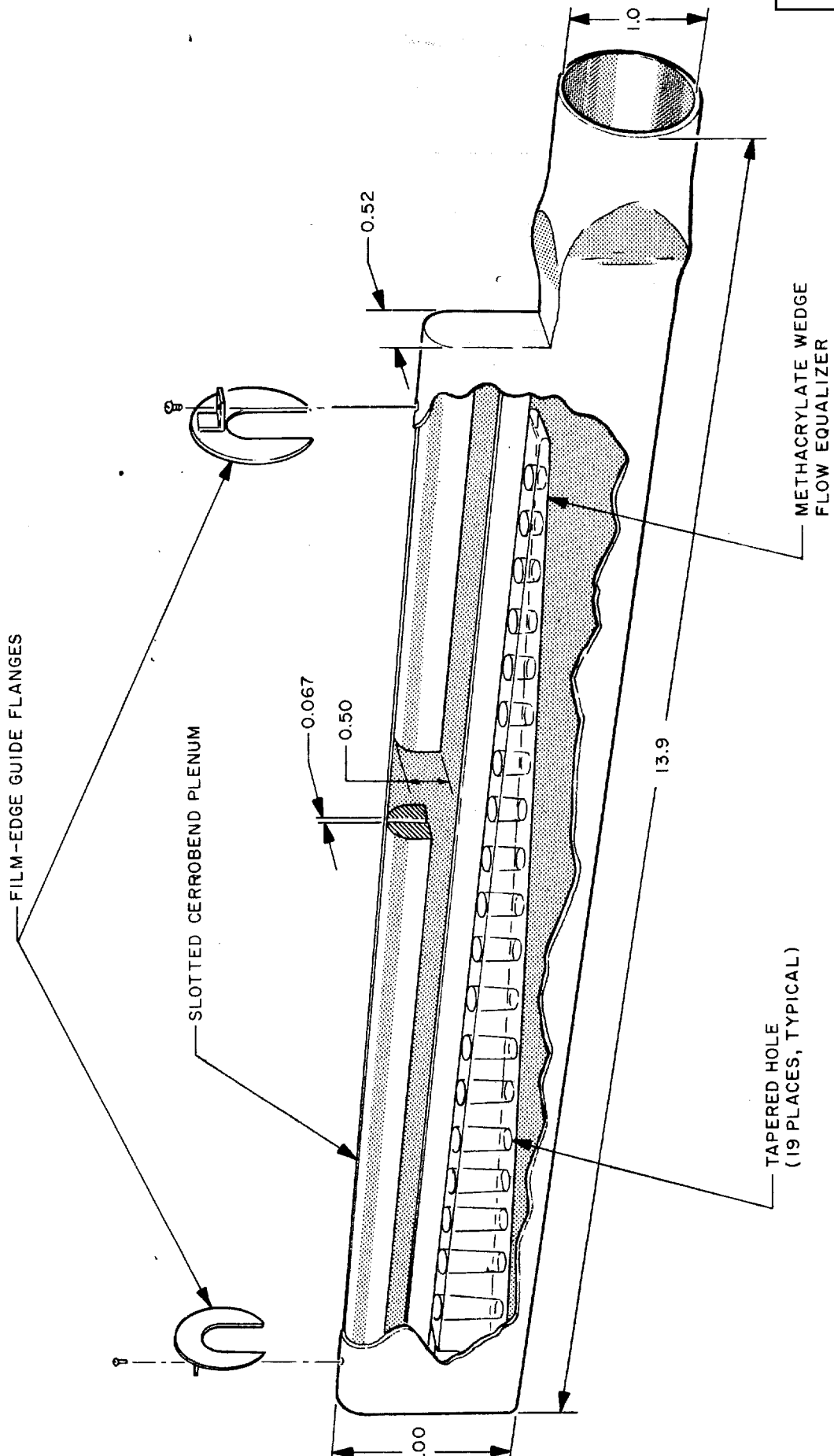


Figure 2-5. Narrow Prototype Liquid Bearing

50075

STAT

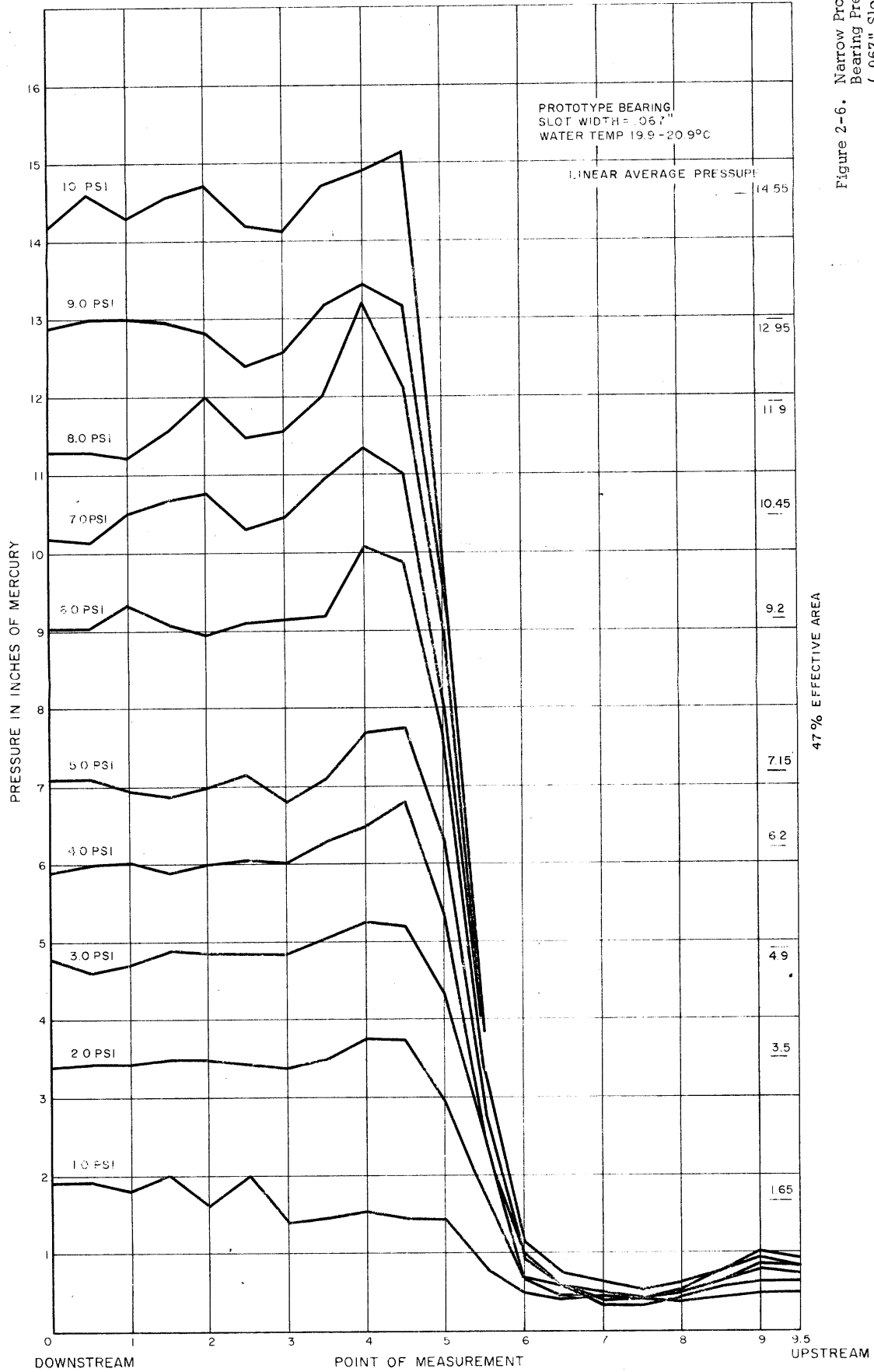


Figure 2-6. Narrow Prototype Liquid Bearing Pressure Profile (.067" Slot)

STAT

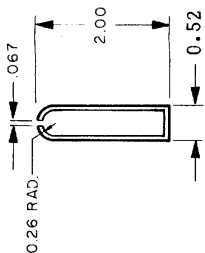
TABLE 2-1
FLOWMETER CALIBRATION DATA AND REYNOLDS NUMBER CALCULATION

Flowmeter Reading gpm	Measured Flow gpm	T ₂ °F	ρ gm/ml	ft ³ /sec	V ft/sec	1/V ² sec ² /ft ²	f	μ lb/ft sec	1/μ ft. sec./lb. /ft ³	ρ lb./ft ³	R _e
41.2	40.8	71.05	.99720	.0893	10.36	.00932	.00218	.000608	1645	62.25	1.11 x 10 ⁵
39.6	40.8	72.55									
37.7	38.2	72.75	.99718	.0833	9.66	.01072	.00214	.000607	1649	62.25	1.04 x 10 ⁵
35.8	38.2	72.85									
33.9	33.8	72.95	.99716	.0724	8.40	.01417	.00215	.000606	1651	62.25	9.05 x 10 ⁴
32.1	31.2	72.45									
30.2	29.6	72.55									
28.3	26.9	72.65	.99716	.0618	7.17	.01945	.00228	.000605	1652	62.25	7.73 x 10 ⁴
26.3	26.3	72.70									
24.4	23.7	72.85									
22.5	21.5	72.90	.99714	.0509	5.90	.02873	.00349	.000605	1654	62.25	6.37 x 10 ⁴
20.6	19.7	73.00									
18.7	18.2	73.10	.99713	.0400	4.64	.04645	.00259	.000604	1655	62.25	5.01 x 10 ⁴
16.7	15.8	73.20									
14.7	13.9	73.30	.99712	.0291	3.38	.08754	.00315	.000603	1657	62.25	3.65 x 10 ⁴
12.8	11.1	73.45									
10.9	10.3	73.50									
9.0	7.9	73.55	.99710	.0182	2.11	.2246	.00332	.000603	1660	62.25	2.29 x 10 ⁴
6.9	7.2	73.65									
4.9	4.5	73.75									
-	2.6	74.05	.99706	.0071	.823	1.476	.00417	.000600	1667	62.25	8.95 x 10 ³

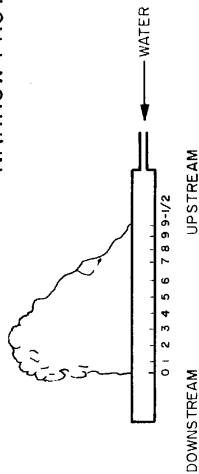
STAT



TABLE 2-2
PRESSURE PROFILE MEASUREMENT DATA FOR
NARROW PROTOTYPE LIQUID BEARINGS



0.062" WALL STAINLESS TUBE
(SIDES FLAT - TOP SEMICIRCULAR)
SLOT WIDTH = .067



P1 psi	Flow gpm	T3 °C	0	1/2	1	1-1/2	2	2-1/2	3	3-1/2	4	4-1/2	5	5-1/2	6	6-1/2	7	7-1/2	8	8-1/2	9	9-1/2
1.0	12.5	19.90	1.89	1.91	1.79	1.99	1.84	1.99	1.87	1.93	2.03	1.99	1.43	.78	.46	.40	.44	.38	.38	.42	.48	.48
2.0	17.0	20.00	3.40	3.44	3.41	3.48	3.48	3.49	3.39	3.49	3.76	3.83	2.93	1.70	.64	.44	.44	.43	.41	.57	.64	.64
3.0	20.5	20.20	4.74	4.60	4.67	4.87	4.84	4.83	4.83	5.05	5.26	5.19	5.35	2.44	1.00	.54	.50	.42	.48	.66	.78	.73
4.0	23.5	17.55	5.91	5.99	6.01	5.88	6.00	6.05	6.01	6.29	6.47	6.79	5.30	2.50	.68	.57	.35	.32	.43	.65	.88	.81
5.0	26.0	18.10	7.07	7.10	6.94	6.86	6.98	7.14	6.80	7.10	7.70	7.73	6.27	2.79	.91	.54	.39	.39	.54	.77	.95	.82
6.0	28.5	18.40	9.04	9.03	9.34	9.08	8.45	9.11	9.15	9.20	10.07	9.88	7.58	3.34	1.14	.72	.64	.51	.61	.77	1.00	.92
7.0	31.0	20.40	10.18	10.13	10.53	10.66	10.76	10.29	10.47	10.92	11.36	10.99	8.09	3.48	1.20	.87	.54	.54	.60	.87	1.05	.92
8.0	32.5	20.50	11.28	11.29	11.23	11.55	11.99	11.47	11.56	12.03	13.22	12.13	8.99	3.94	1.05	1.05	.65	.48	.65	.97	1.23	.98
9.0	34.5	20.70	12.90	12.98	13.03	12.95	12.81	12.38	12.58	13.16	13.43	13.17	9.52	3.85	1.43	1.15	.88	.67	.64	.65	1.27	1.08
10.0	36.3	20.90	14.18	14.58	14.27	14.56	14.70	14.20	14.13	14.71	14.89	15.13	9.79	3.53	.91	1.11	.81	.66	.64	.68	1.34	1.06

TABLE 2-3
WITH CERROBEND AND METHACRYLATE WEDGE IN PLENUM

P1 psi	Flow gpm	T3 °C	0	1/2	1	1-1/2	2	2-1/2	3	3-1/2	4	4-1/2	5	5-1/2	6	6-1/2	7	7-1/2	8	8-1/2	9	9-1/2
0.5		19.60	.59	.52	.52	.46	.44	.42	.05	0	.05	.27	.32	.40	.41	.46	.51	.39	.25	.15	.10	.10
1.0		19.85	1.28	1.23	1.27	1.04	1.16	1.02	1.05	1.02	.45	1.07	1.24	1.04	1.03	.93	1.37	1.19	.80	.60	.42	.34
1.5		20.65	2.75	2.56	2.45	2.65	1.73	2.21	2.43	2.75	2.70	2.94	2.90	.88	2.62	2.07	2.81	2.97	2.02	1.49	.83	.95
2.0		20.95	3.43	3.55	3.25	3.63	2.35	3.09	3.27	3.75	3.69	3.76	3.87	3.17	3.63	3.15	3.87	3.29	3.02	2.17	1.68	1.66
3.0		21.10	4.81	5.21	5.06	5.54	3.51	4.78	3.81	5.49	5.53	5.46	5.61	5.81	5.34	5.41	5.58	5.52	3.81	2.59	1.89	1.90
4.0		21.20	6.77	6.99	6.39	5.94	4.15	5.99	6.73	6.81	6.79	6.31	6.05	6.70	6.70	6.66	6.97	6.15	5.54	3.82	2.79	2.80

*Chip in Rotameter made these readings suspect

The outside dimensions of the plenum chamber were 11.57 inches long, 2.00 inches deep, and 0.52 inches wide, with a wall thickness of 0.062 inch. The sides and bottom of the plenum were rectangular and the top semicircular. The bearing had a single slot 9.56 inches long and 0.067 inch wide.

The series of experiments and test data gathered in this report were confined to bearings having a single slot and to one bearing having three slots. As discussed in Section 1, patterns of holes in liquid bearings have inherent disadvantages such as excess power consumption, energy losses, inefficiencies, and streaking of film. It appeared obvious that a slot would obviate many of these drawbacks, particularly that of streaking due to local development.

All pressure profiles were made by sampling the slot width at 1/2-inch intervals with the pitot tube attached to the inclined manometer. (The first pitot used was a modified assayer's blowpipe.) The static pressures obtained were recorded, together with the inlet gage pressure, the flow in gpm, and the water temperature in degrees centigrade. All air was bled from the test lines prior to measurement and repeatability to ± 1 percent accuracy was checked by duplicating runs on different days.

If a fluid is injected into one end of a closed straight tube of any constant cross-section and allowed to escape through a single long narrow slot, the shape of the resultant fluid fall is roughly parabolic (Figure 2-7). This effect is pronounced where the cross-sectional area is in the range of one square inch and gradually disappears as the area is increased. Thus, if the parabola were graphed in the first and fourth quadrants, in rectangular coordinates with the base lying along the ordinate axis, the apex would fall on the abscissa. Considering the first quadrant only, the apex (or $Y = 0$ point) would appear at the upstream end of the slot and the highest

(Continued page 2-12)

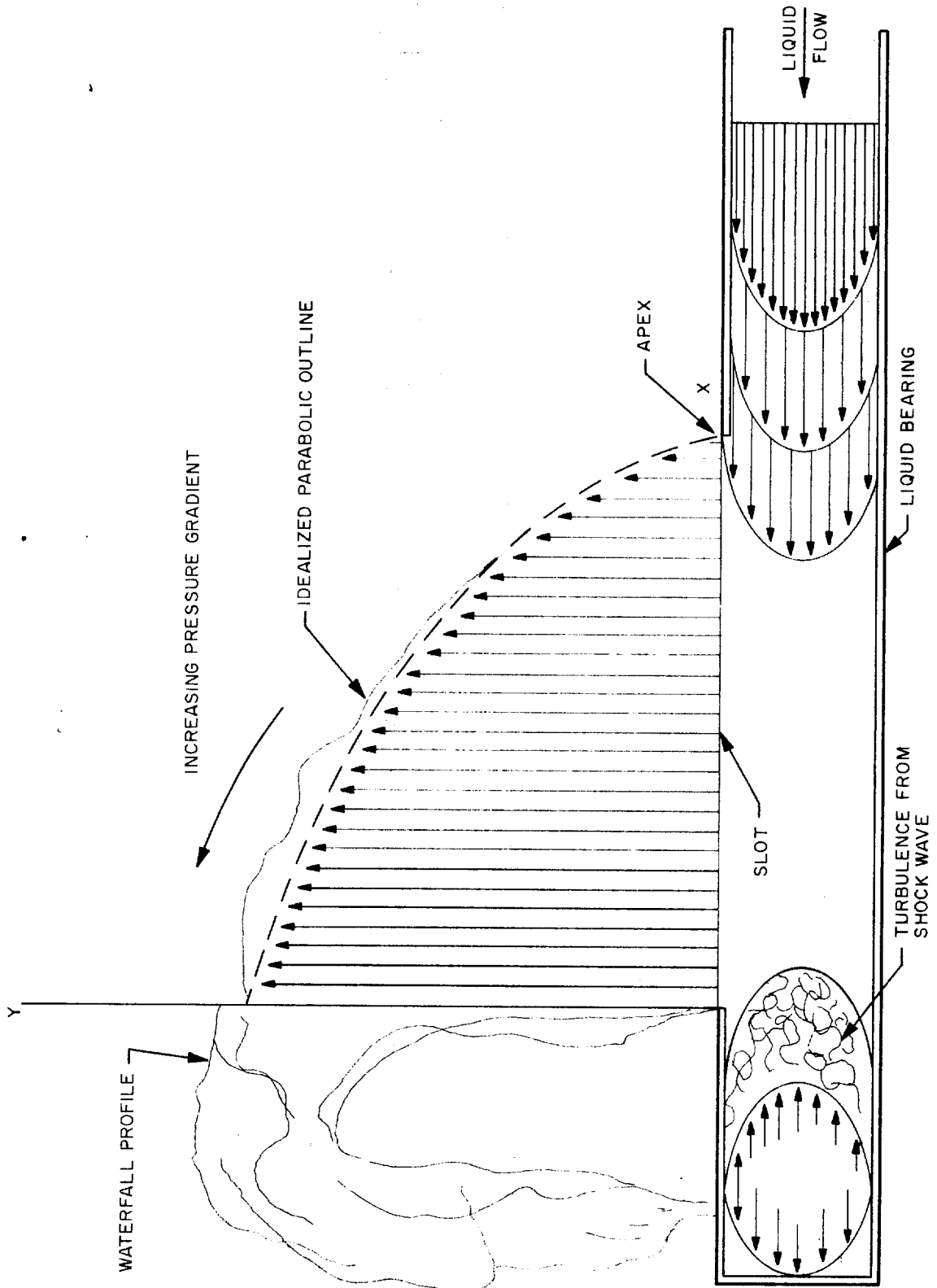


Figure 2-7. Analysis of Pressure-Flow Relationship

50077

point of the leg (or $X = 0$ intersection) at the downstream end. This latter was also the point of highest pressure as can be readily observed from a typical pressure profile plot.

Analytically, the effect can be explained by examining the pressure-flow relationship diagrammed. Apparently, the shock wave generated as the fluid enters is transmitted to a pressure gradient by impingement on the far end of the bearing. This unequal gradient then gives the characteristic shape to the profile.

The plot diagrammed in Figure 2-6 also shows a sharp fall-off of pressure about midway on the slot. Since uneven pressure causes a tipping of the film and skidding away from the pressure area, this condition could not be tolerated. In order to compensate for the unbalanced pattern, a methacrylate plastic wedge was designed to fit inside the bottom of the plenum with its wide end downstream as shown in Figure 2-5.

The wedge was 9.94 inches long, 0.41 inch wide, and tapered from 0.60 to 0.125 inch. It was drilled with 19 holes 0.196 inch in diameter; each hole was tapered with a No. 120 Ace reamer (0.498 to 0.119 inch in 3.53 inches). When this was mounted in the plenum so that the fluid was forced to flow from the small to the large ends of the tapered holes, the pressure profile was somewhat improved. However, there were still unacceptable eccentricities in the pattern. At this point, Cerrobend was added to the inside of the semicircular portion of the plenum to extend the throat of the slot to a 1/2-inch depth. Such a bearing, with a double plenum, had previously given an improved pattern. No significant change was noted; the general pattern was still subject to peaks and valleys (Figure 2-8 and Table 2-3).

(Continued page 2-14

STAT

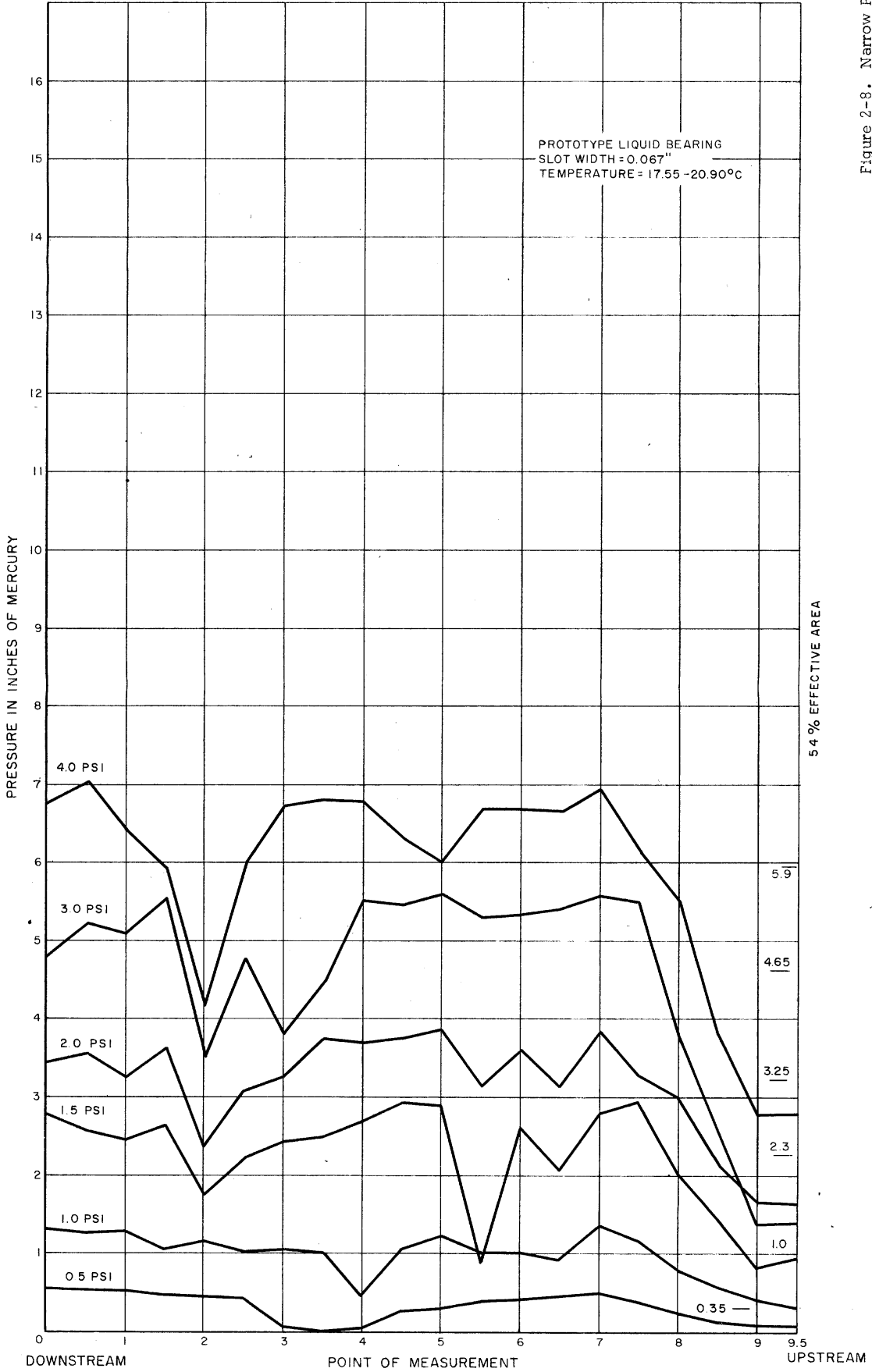


Figure 2-8. Narrow Prototype Liquid Bearing with Cerrobend Plenum and Plastic Wedge 2-13

Various attempts to equalize the flow were unsuccessful. These included masking the tapered slots with cellular polyurethane foam, filing lips on the upstream tapered nozzles in the equalizer, increasing the diameter of the upstream tapered nozzles, and changing the position of the equalizer one inch toward the upstream end of the bearing.

The test sequence was repeated on a similar type of bearing, differing in slot width. The slot, in this case, was 9.52 inches long by 0.120 inch wide. While considerably higher flow rates were necessary to duplicate the inlet pressure obtained with the narrow slotted bearing, the pressure profile without an equalizer was almost identical (Figure 2-9 and Table 2-4). The fact that no significant difference appeared in the plots obtained permits the following hypothesis.

Liquid bearings having an identical cross-sectional configuration and area will produce a characteristic pressure profile plot whose magnitude at constant inlet pressure is directly proportional to flow. Further experimentation with the narrow bearings was abandoned, not only because of the difficulty of equalizing the flow, but also because of a more significant drawback. This drawback proved to be that the extra force required to bend film and leader of heavier base thicknesses (5 to 7 mils) around the narrow radii used more energy (reflected in increased gpm) than was saved by the economies inherent in the bearings. If, on the other hand, the most important of the design criteria were the size of the processor, the narrow bearing might prove to be the only possible trade-off.

2.2.2 Liquid Bearing Slot Data

To thoroughly explore the complex relationships between pressure profiles, throat/plenum area ratios, inlet pressures, and rates of flow, five experimental stainless-steel bearings were built. Slots were identical, 0.063 by 9-1/2 inches, and so were tube lengths. Only the inside diameter

(Continued page 2-17)

STAT

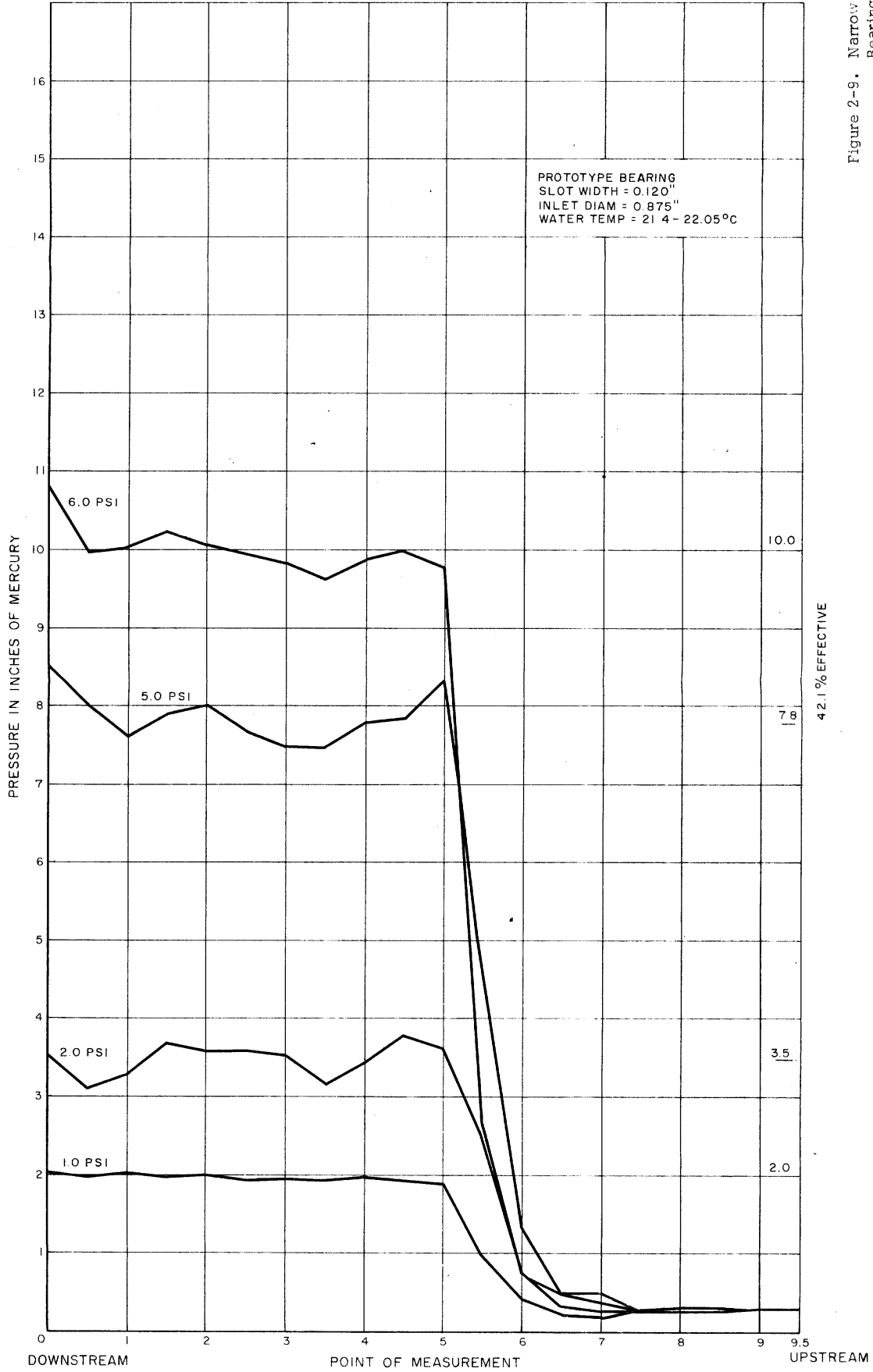
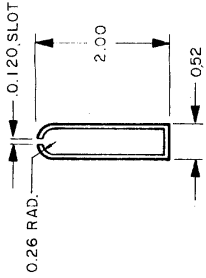


Figure 2-9. Narrow Prototype Liquid Bearing with Wide Slot

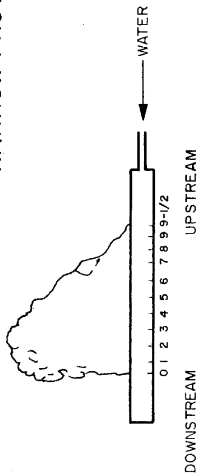
2-15

STAT

TABLE 2-4
PRESSURE PROFILE MEASUREMENT DATA FOR
NARROW PROTOTYPE LIQUID BEARINGS



.062" WALL STAINLESS TUBE
(SIDES FLAT - TOP SEMICIRCULAR)
SLOT WIDTH = .120"



P1 psi	Flow gpm	T3 °C	0	1/2	1	1-1/2	2	2-1/2	3	3-1/2	4	4-1/2	5	5-1/2	6	6-1/2	7	7-1/2	8	8-1/2	9	9-1/2	
1.0	19.0	21.40	2.01	1.98	2.02	1.97	2.02	1.95	1.97	1.93	1.99	1.96	1.91	.99	.43	.23	.20	.29	.27	.27	.30	.30	.30
2.0	25.0	21.85	3.51	3.11	3.29	3.71	3.60	3.62	3.55	3.19	3.41	3.80	3.64	2.54	.78	.32	.28	.28	.29	.32	.33	.33	.31
5.0	41.0	21.90	8.51	8.01	7.61	7.88	8.01	7.69	7.50	7.48	7.78	7.85	8.32	4.47	1.36	.51	.52	.33	.27	.26	.23	.27	.27
6.0	46.5	22.05	10.80	9.97	10.20	10.25	10.08	9.98	9.83	9.62	9.89	9.98	9.76	2.65	.75	.53	.42	.33	.27	.25	.26	.26	.30

TABLE 2-5
.065" WALL STAINLESS TUBE
(WELDED AND DRAWN)
INSIDE DIAMETER = .1000"
SLOT WIDTH = .063"

P1 psi	Flow gpm	T3 °C	0	1/2	1	1-1/2	2	2-1/2	3	3-1/2	4	4-1/2	5	5-1/2	6	6-1/2	7	7-1/2	8	8-1/2	9	9-1/2	
1.0	18.0	21.10	2.37	2.43	2.47	2.46	2.46	2.46	2.52	2.37	2.39	2.38	2.39	2.44	2.24	2.14	2.14	2.10	1.97	1.88	1.88	.49	.49
2.0	24.9	20.92	4.54	4.54	4.53	4.53	4.62	4.62	4.58	4.47	4.38	4.31	4.35	4.19	4.17	4.20	3.74	3.88	3.95	3.78	3.73	3.54	3.54
3.0	30.8	21.60	6.96	6.93	6.56	6.97	6.88	6.81	6.71	6.89	6.92	6.60	6.73	6.73	6.56	6.59	6.22	6.21	5.66	5.51	6.18	6.10	6.10
4.0	34.0	22.00	8.39	8.45	8.39	8.74	8.76	8.73	8.70	8.58	8.70	8.15	8.17	8.12	8.15	7.36	7.31	7.73	7.02	7.54	7.26	6.04	6.04
5.0	37.7	22.40	10.85	10.74	10.72	10.64	10.84	10.80	10.68	10.59	10.37	10.14	10.47	9.33	9.54	9.61	9.61	8.76	8.53	8.26	8.81	7.76	7.76
6.0	41.5	22.80	12.76	12.69	12.78	12.78	12.88	12.78	12.41	12.51	12.67	12.73	12.67	11.88	11.01	11.15	11.15	10.88	10.96	10.41	10.21	10.08	10.08
6.75	45.8	22.40	15.00	14.75	14.90	15.17	15.39	15.17	15.04	15.06	14.90	14.65	14.07	13.90	13.51	12.75	12.75	12.72	12.05	11.95	10.11	10.53	10.53

was varied. The nominal inside diameters were 1.000, 1.250, 1.500, 1.620, and 1.875 inches (Figure 2-10). The material was welded and drawn tubing selected because it is less expensive than the seamless and polished type and is normally stocked in [] raw stores. STATINTL These were "run-of-the-shop" jobs and no particular stress was placed upon dressing the milled slots after machining.

Pressure profiles were measured on each bearing and then graphed (Figures 2-11, 2-12, 2-13, 2-14, and 2-15, and Tables 2-5, 2-6, 2-7, 2-8, and 2-9). The construction material, the machine finish of the slot, and the position of the seam relative to the slot appeared to be much more critical parameters than was supposed. When the empirical data obtained on all bearings were grouped on one graph, the differences became apparent (Figure 2-16).

The most and the least satisfactory bearings from the standpoint of economy of fluid flow were the two narrow prototypes discussed in Section 2.2.1. However, since the effective area available for the cushion support of film was only 47 and 42 percent respectively for these bearings, the results should not be misinterpreted. The five experimental stainless-steel bearings were grouped rather closely and differed mainly in their effective support areas. The fact that the curve for the 1.620 inch inside diameter bearing falls to the left of those for the 1.500 and the 1.875 inch inside diameter bearings supports the statement concerning the critical nature of some of the parameters.

The 1.500 inch inside diameter copper bearing discussed in Subsection 2.2.3 following, proved to be the most satisfactory compromise among the parameters.

(Continued page 2-27)

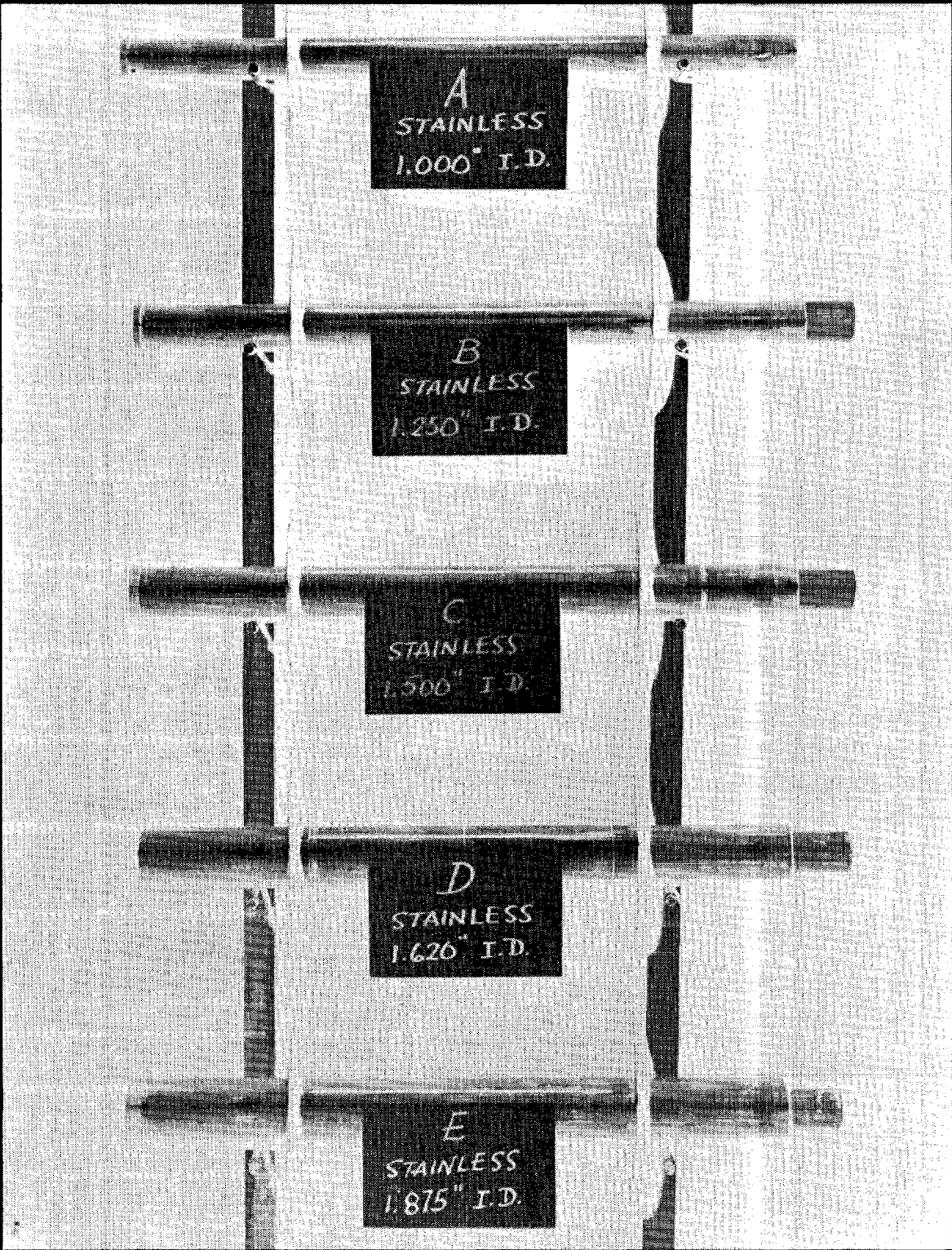


Figure 2-10. Five Stainless-Steel Bearings - All Slots 0.063 x 9-1/2 Inches

STAT

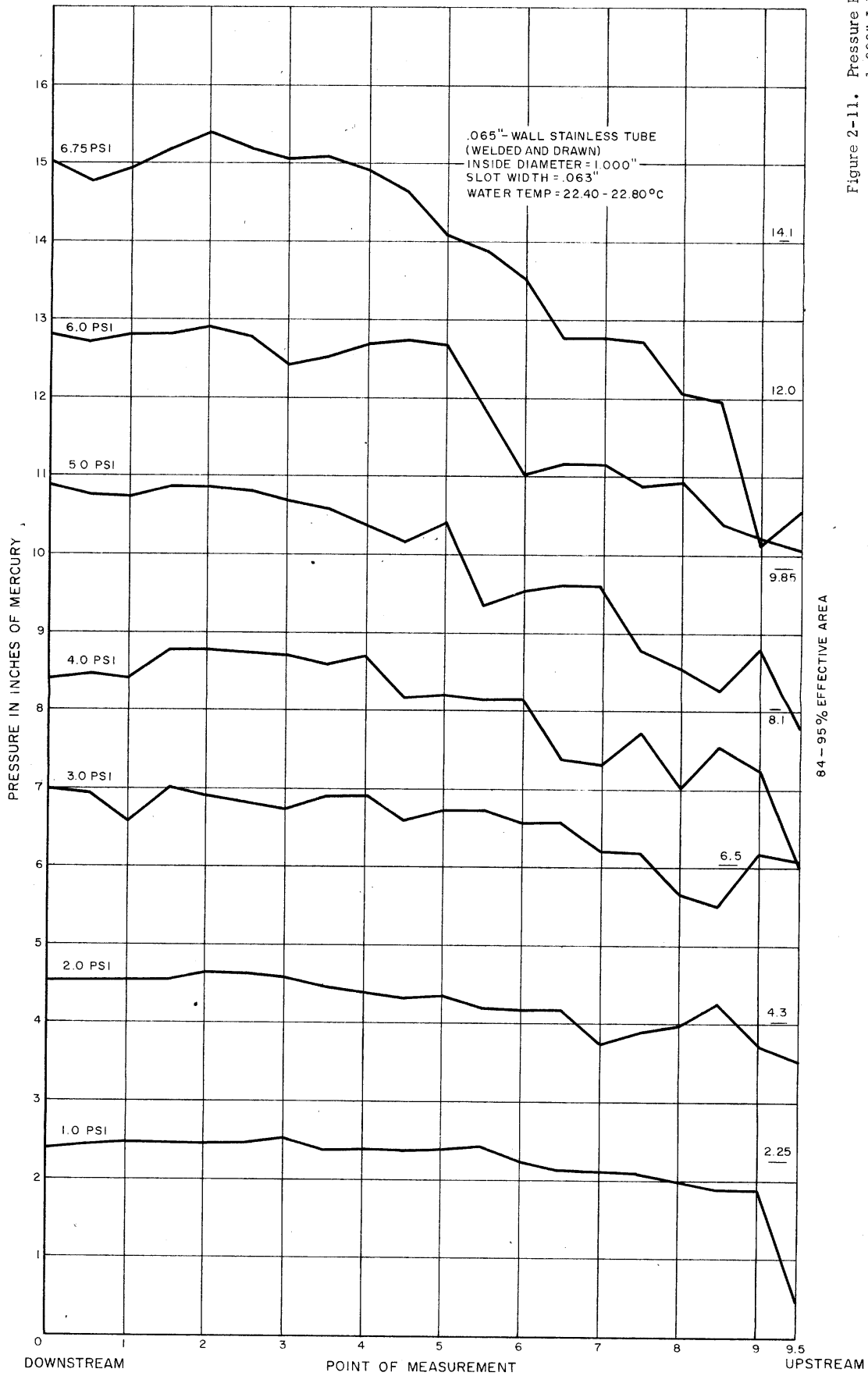


Figure 2-11. Pressure Profile for 1.000" I.D. Circular Stainless Bearing

STAT

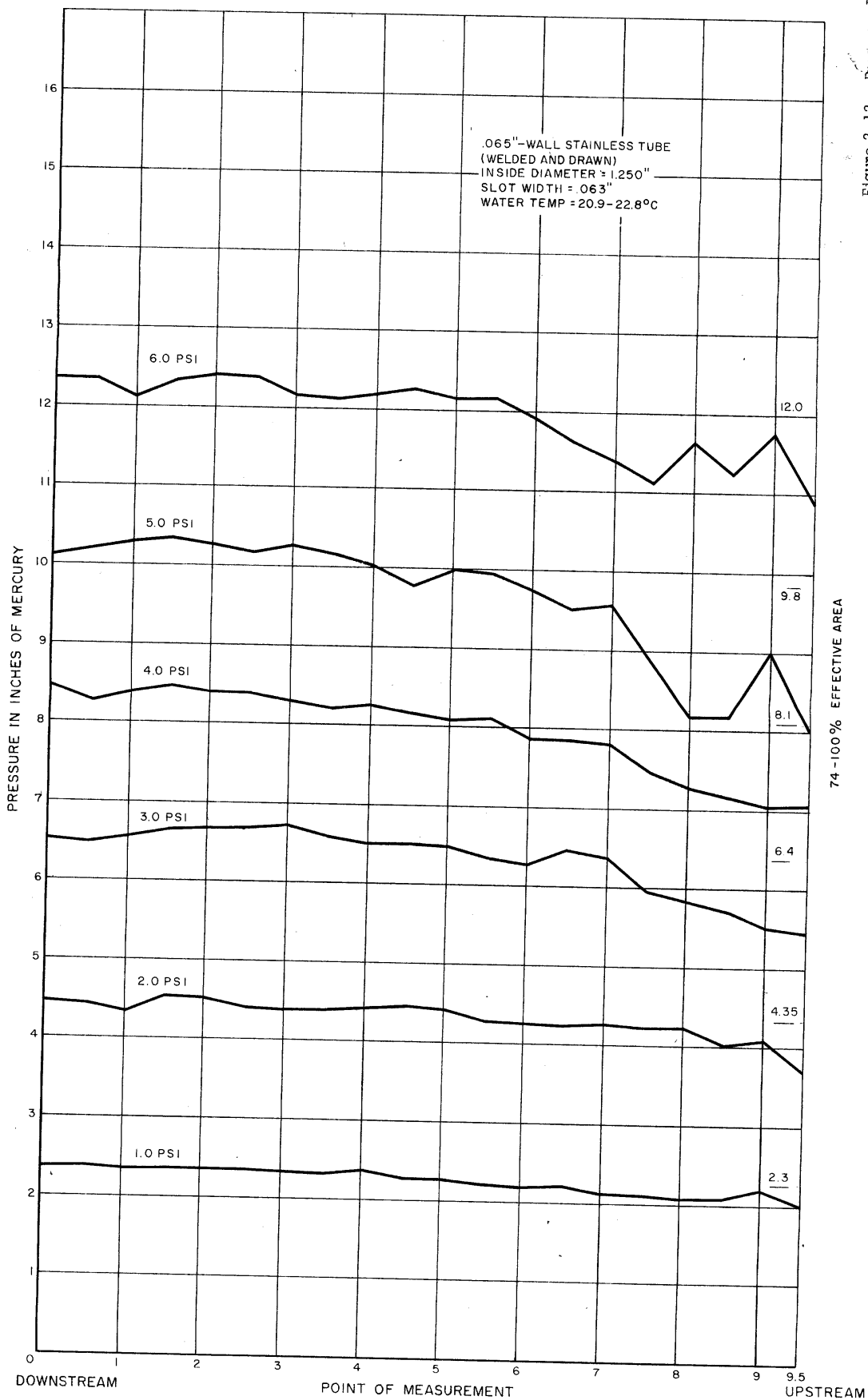
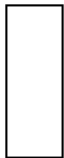


Figure 2-12. Pressure Profile for 1.250" I.D. Circular Stainless Bearing

2-20

STAT

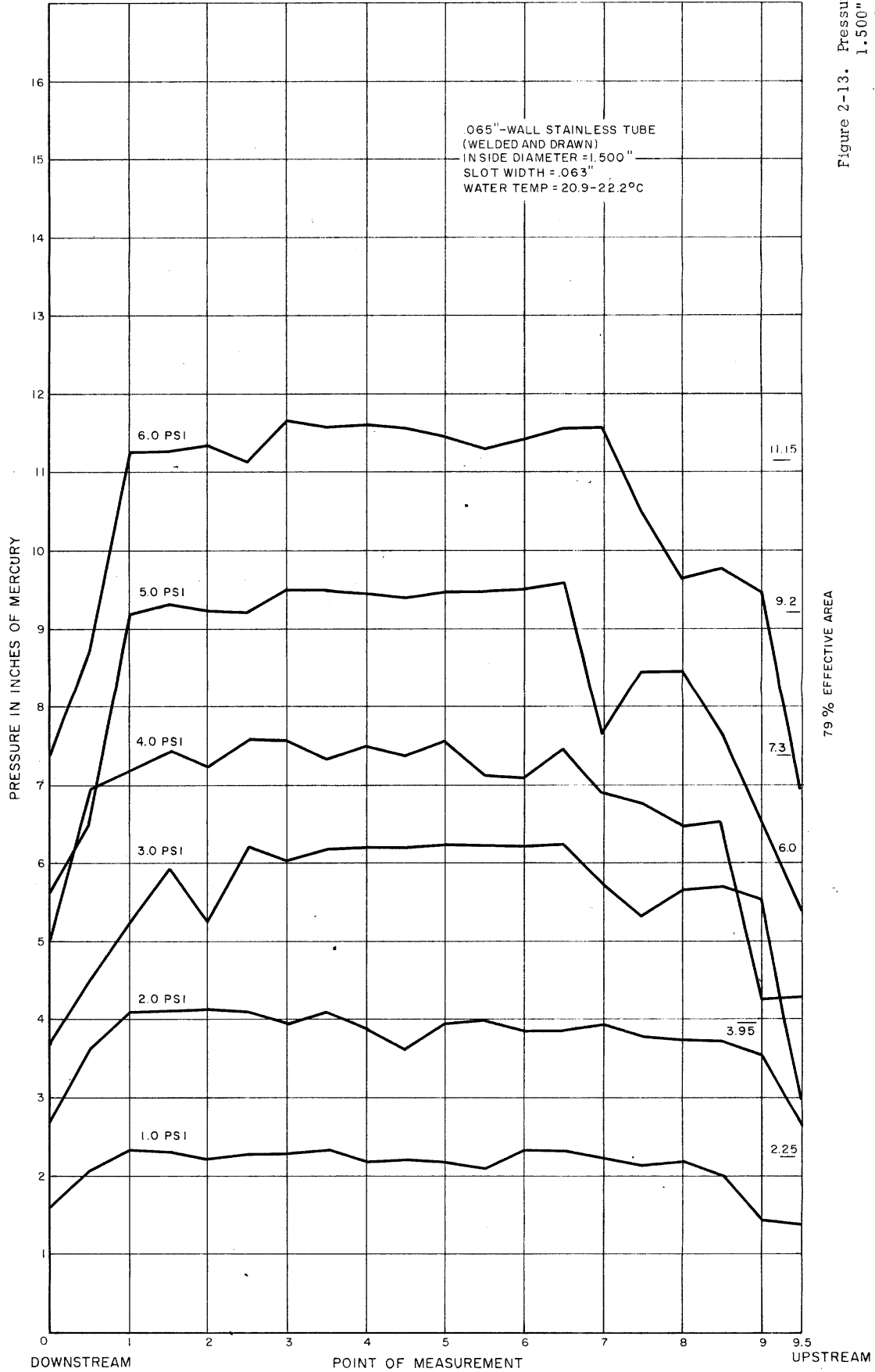


Figure 2-13. Pressure Profile for 1.500" I.D. Circular Stainless Bearing

2-21

STAT

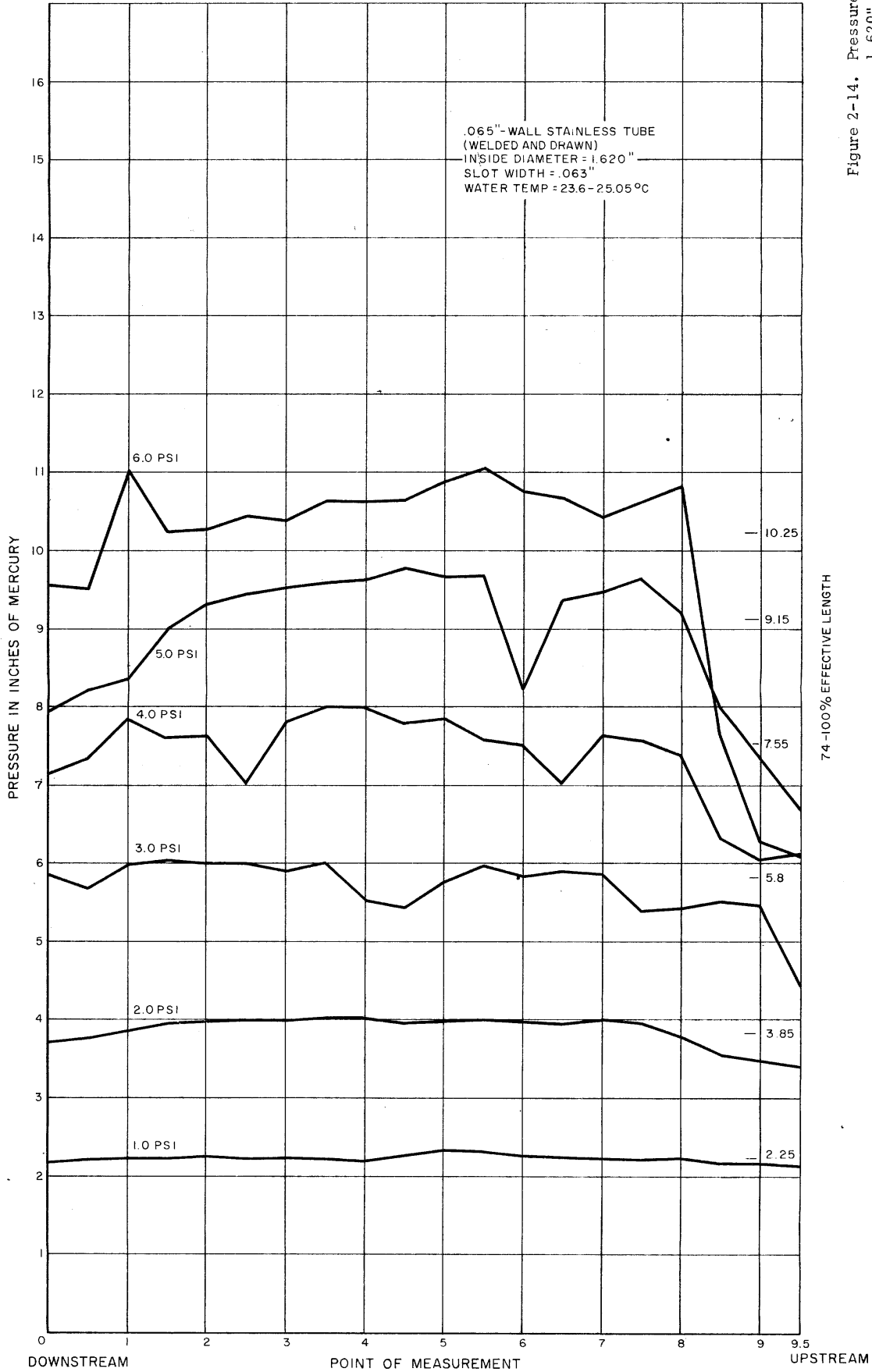


Figure 2-14. Pressure Profile for
1.620" I.D. Circular
Stainless Bearing

STAT

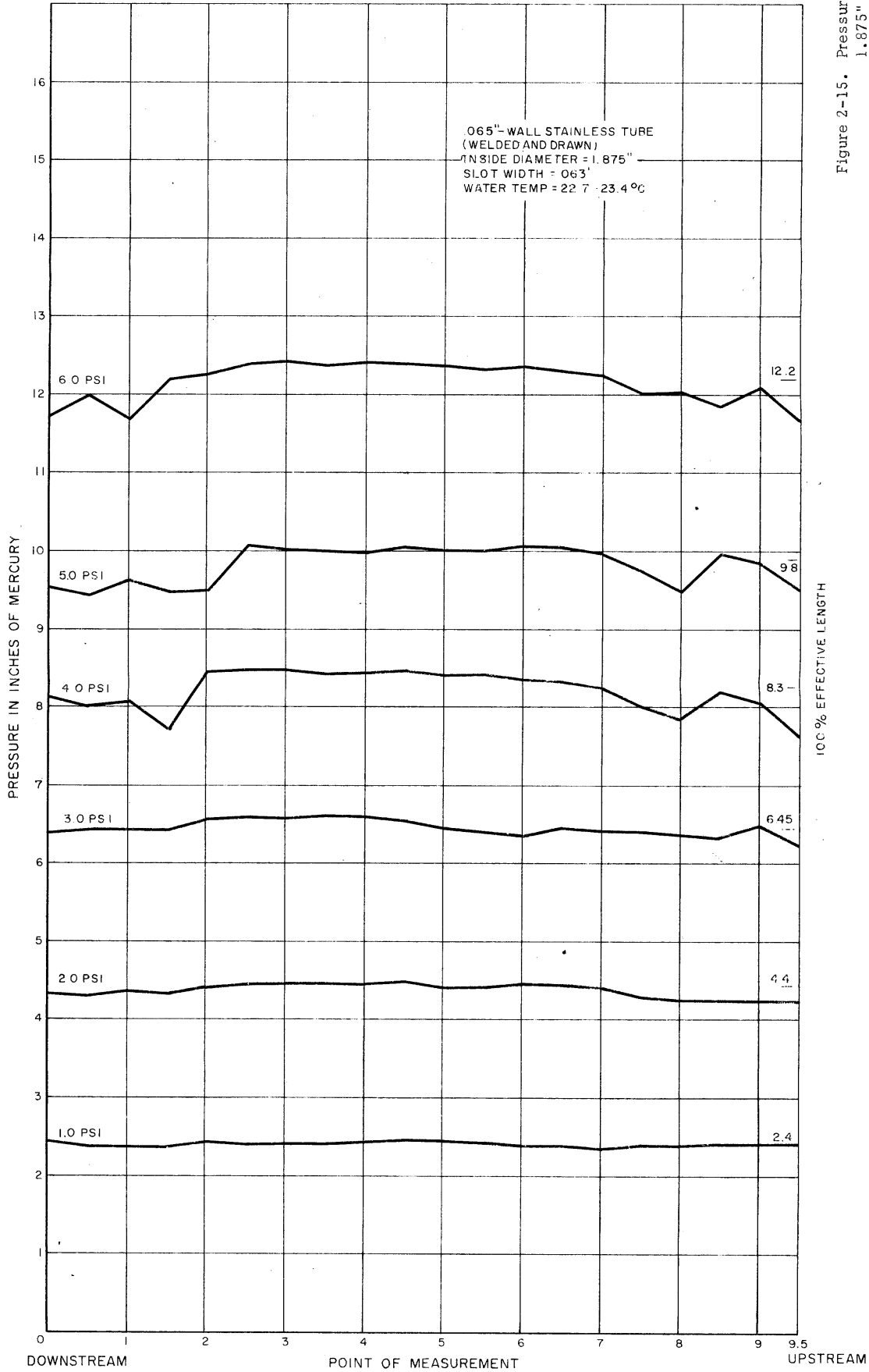
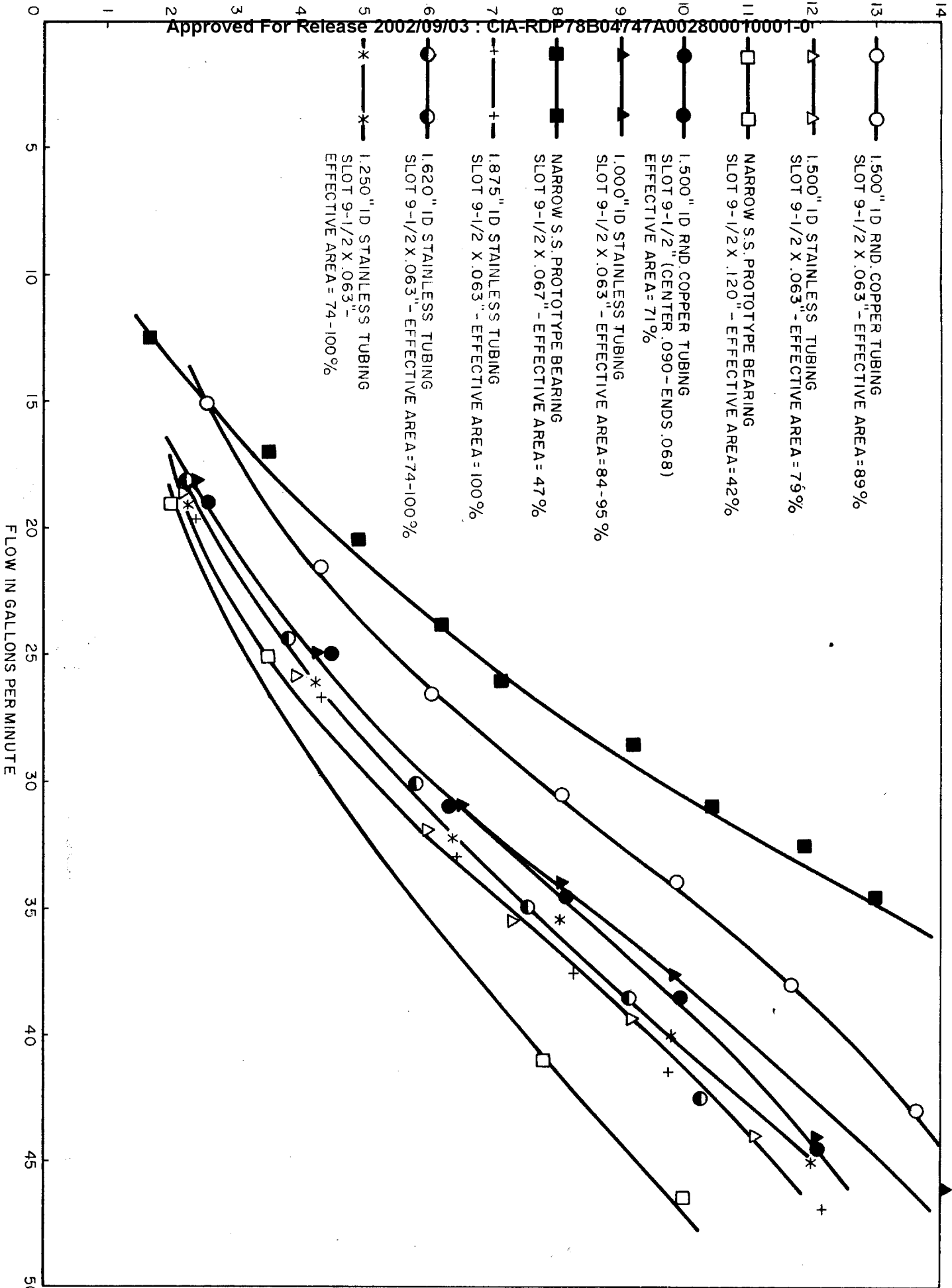


Figure 2-15. Pressure Profile for 1.875" I.D. Circular Stainless Bearing

2-23

PRESSURE IN INCHES OF MERCURY

Approved For Release 2002/09/03 : CIA-RDP78B04747A002800010001-0



Approved For Release 2002/09/03 : CIA-RDP78B04747A002800010001-0

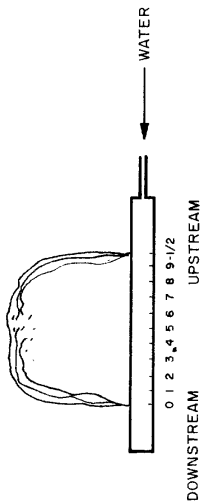
Figure 2-16. Pressure vs. Flow for Experimental Bearings

STAT

STAT



**TABLE 2-6
PRESSURE PROFILE MEASUREMENT DATA
FOR CIRCULAR CROSS-SECTION LIQUID BEARING**



.065" WALL STAINLESS TUBE
(WELDED AND DRAWN)
INSIDE DIAMETER = 1.250"
SLOT WIDTH = .063"

P psi	Flow gpm	T ₃ °C	0	1/2	1	1-1/2	2	2-1/2	3	3-1/2	4	4-1/2	5	5-1/2	6	6-1/2	7	7-1/2	8	8-1/2	9	9-1/2
1.0	18.8	22.60	2.40	2.41	2.39	2.40	2.40	2.39	2.38	2.36	2.41	2.31	2.30	2.26	2.23	2.25	2.17	2.14	2.10	2.12	2.23	2.05
2.0	26.1	22.80	4.98	4.96	4.37	4.58	4.54	4.44	4.41	4.42	4.45	4.48	4.45	4.31	4.29	4.27	4.24	4.25	4.25	4.06	4.11	3.73
3.0	32.1	20.90	6.54	6.50	6.58	6.66	6.69	6.71	6.73	6.61	6.52	6.53	6.50	6.36	6.30	6.49	6.40	5.98	5.86	5.74	5.53	5.47
4.0	35.3	21.10	8.42	8.29	8.41	8.48	8.42	8.42	8.31	8.23	8.29	8.19	8.11	8.14	7.89	7.87	7.82	7.50	7.30	7.19	7.06	7.09
5.0	40.1	21.30	10.14	10.21	10.31	10.36	10.23	10.19	10.28	10.19	10.04	9.80	9.95	9.97	9.76	9.64	9.61	8.88	8.20	8.19	9.02	8.58
6.0	45.0	21.70	12.39	12.38	12.15	12.35	12.43	12.40	12.19	12.15	12.20	12.28	12.17	12.18	11.94	11.65	11.41	11.14	11.67	11.27	11.72	10.91

.065" WALL STAINLESS TUBE
(WELDED AND DRAWN)
INSIDE DIAMETER = 1.500"
SLOT WIDTH = .063"

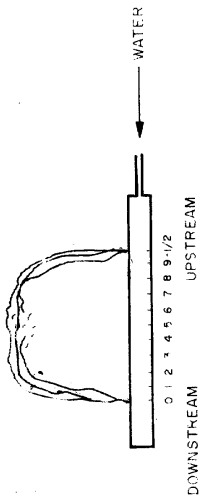
TABLE 2-7

P psi	Flow gpm	T ₃ °C	0	1/2	1	1-1/2	2	2-1/2	3	3-1/2	4	4-1/2	5	5-1/2	6	6-1/2	7	7-1/2	8	8-1/2	9	9-1/2
1.0	18.7	21.10	1.61	2.09	2.33	2.31	2.22	2.30	2.30	2.36	2.19	2.23	2.19	2.11	2.33	2.34	2.22	2.13	2.18	2.01	1.45	1.39
2.0	25.8	21.50	2.70	3.63	4.10	4.12	4.13	4.11	3.96	4.10	3.89	3.63	3.97	3.98	3.87	3.87	3.94	3.79	3.74	3.72	3.57	2.69
3.0	31.8	21.80	3.74	4.52	5.24	5.93	5.29	6.23	6.04	6.19	6.22	6.21	6.25	6.24	6.23	6.26	5.73	5.37	5.65	5.70	5.54	3.01
4.0	35.5	20.90	5.06	6.96	7.19	7.44	7.24	7.58	7.56	7.34	7.50	7.38	7.56	7.14	7.10	7.48	6.91	6.76	7.00	7.06	4.27	4.30
5.0	39.3	22.00	5.69	6.50	9.18	9.32	9.22	9.21	9.51	9.51	9.45	9.40	9.47	9.47	9.52	9.62	7.68	8.45	8.48	7.70	6.54	5.41
6.0	44.0	22.20	7.43	8.71	11.25	11.33	11.13	11.65	11.57	11.57	11.61	11.56	11.46	11.29	11.42	11.55	11.58	10.46	9.65	9.78	9.50	6.96

63
2-25

STAT

TABLE 2-8
PRESSURE PROFILE MEASUREMENT DATA
FOR CIRCULAR CROSS-SECTION LIQUID BEARING



0.065" WALL STAINLESS TUBE
 (WELDED AND DRAWN)
 INSIDE DIAMETER = 1.620"
 SLOT WIDTH = .063"

P ₁ psi	Flow gpm	T ₃ °C	0	1/2	1	1-1/2	2	2-1/2	3	3-1/2	4	4-1/2	5	5-1/2	6	6-1/2	7	7-1/2	8	8-1/2	9	9-1/2
1.0	18.2	23.60	2.18	2.22	2.24	2.24	2.27	2.25	2.26	2.25	2.22	2.28	2.36	2.34	2.28	2.27	2.25	2.24	2.25	2.18	2.19	2.17
2.0	24.4	23.90	3.70	3.77	3.88	3.92	3.99	4.00	3.99	4.02	4.03	3.98	4.00	4.03	3.99	3.97	4.01	3.98	3.81	3.57	3.50	3.43
3.0	30.1	24.20	5.85	5.69	5.99	6.04	6.01	5.90	5.91	6.02	5.53	5.44	5.78	5.99	5.86	5.92	5.90	5.40	5.44	5.54	5.50	4.50
4.0	34.9	24.40	7.15	7.33	7.84	7.60	7.63	7.05	7.83	8.00	7.98	7.79	7.87	7.60	7.53	7.04	7.70	7.59	7.41	6.35	6.57	6.14
5.0	38.5	24.65	7.93	8.21	8.36	9.02	9.32	9.45	9.53	9.61	9.64	9.79	9.68	99.65	8.24	9.38	9.48	8.67	9.24	7.99	7.35	6.74
6.0	42.5	25.05	9.53	9.50	11.04	10.04	10.27	10.45	10.39	10.64	10.62	10.65	10.89	11.06	10.77	10.69	10.45	10.65	10.84	7.69	6.30	6.12

0.065" WALL STAINLESS TUBE
 (WELDED AND DRAWN)
 INSIDE DIAMETER = 1.875"
 SLOT WIDTH = .063"

TABLE 2-9

P ₁ psi	Flow gpm	T ₃ °C	0	1/2	1	1-1/2	2	2-1/2	3	3-1/2	4	4-1/2	5	5-1/2	6	6-1/2	7	7-1/2	8	8-1/2	9	9-1/2
1.0	19.6	22.7	2.40	2.35	2.35	2.35	2.43	2.40	2.41	2.41	2.45	2.48	2.46	2.44	2.40	2.41	2.35	2.40	2.40	2.42	2.42	2.43
2.0	26.6	22.9	4.32	4.28	4.34	4.31	4.41	4.45	4.45	4.47	4.46	4.48	4.41	4.42	4.57	4.45	4.41	4.29	4.25	4.25	4.24	4.24
3.0	32.8	23.1	6.36	6.42	6.42	6.42	6.55	6.57	6.56	6.60	6.58	6.54	6.45	6.40	6.35	6.45	6.92	6.92	6.36	6.32	6.49	6.23
4.0	37.4	23.4	8.10	7.96	8.04	7.58	8.43	8.46	8.46	8.41	8.42	8.25	8.39	8.40	8.33	8.30	8.23	8.00	7.83	8.19	8.04	7.62
5.0	41.3	23.2	9.51	9.41	9.61	9.45	9.48	10.07	10.00	9.99	9.96	10.03	10.01	10.00	10.05	10.03	9.96	9.75	9.98	9.96	9.84	9.51
6.0	46.8	23.4	11.62	11.93	11.65	12.17	12.22	12.37	12.41	12.36	12.41	12.39	12.37	12.32	12.35	12.28	12.23	12.01	12.02	11.85	12.08	11.63

2.2.3 Self-Centering Liquid Bearings

In the list of experimental objectives, one important aim was to produce a liquid or air bearing that would tend to keep the film centered while it travelled through the processor, regardless of minor bearing misalignments. In the ideal configuration embodying this principle, the edge guides would be eliminated.

To attain this objective, a simple, single-slot bearing was built from smooth, polished copper. Its length was 20-1/4 inches; the inside diameter was 1.500 inches \pm .005 inch, and the slot was 9-1/2 inches by 0.063 inch. The pressure profile was carefully measured (Figure 2-17 and Table 2-10) and the bearing was modified as discussed below.

Many years ago most machine tools were belt-driven by a series of overhead pulleys connected to a central power source. These pulleys were cylindrical, with a slight crown to keep the belts centered. Applying this principle directly to the liquid bearing problem, a unit was produced whose maximum liquid pressure was at the center. This was done by utilizing the parabolic principle previously discovered with the narrow bearings (see Figure 2-7). By selecting a tube of such size that its internal cross-sectional area was equal to the annular area between its outside diameter and the inside diameter of the main bearing tube, the objective was accomplished. When the smaller tube was mounted on a solid bulkhead located midway on the slot and water was injected in one end, fluid flowing in the annular area formed a parabola toward the center, while fluid flowing through the inner pipe was forced to reverse its direction at the downstream end, forming a second parabola which met the first one at the center. The combined flow created a high-pressure area at the center of the slot and its waterfall pattern was extremely symmetrical.

(Continued page 2-30)

STAT

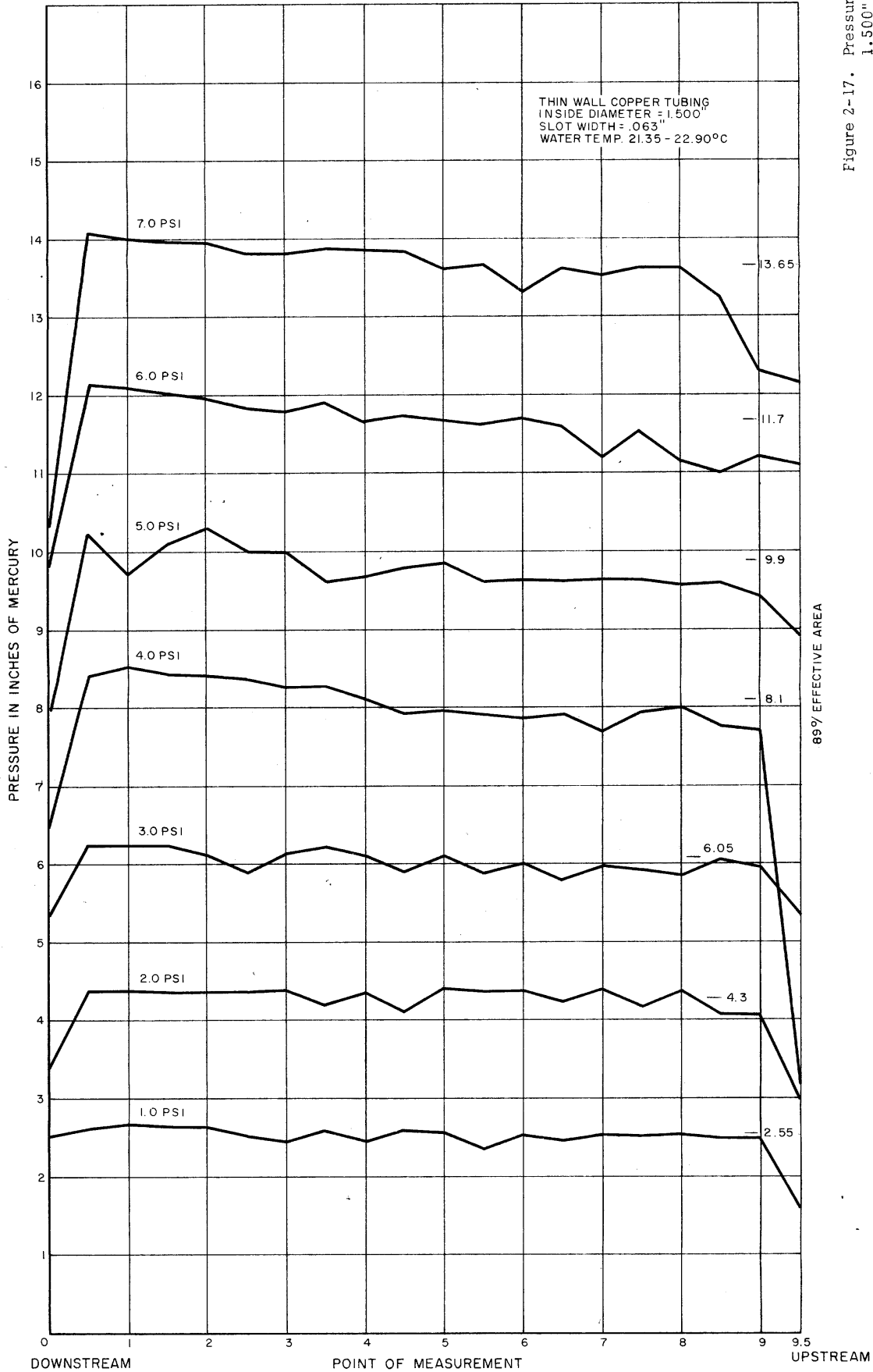
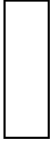


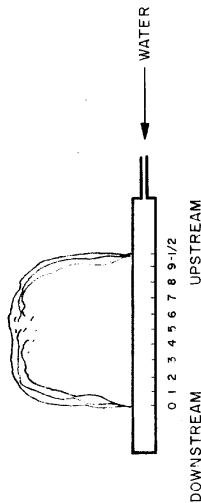
Figure 2-17. Pressure Profile for 1.500" I.D. Circular Copper Bearing

51 2-28

STAT



TABLE 2-10
PRESSURE PROFILE MEASUREMENT DATA
FOR CIRCULAR CROSS-SECTION LIQUID BEARING



.065" WALL COPPER TUBE
 (SEAMLESS)
 INSIDE DIAMETER = 1.500" ± 0.005
 SLOT WIDTH = .063"

P ₁ psi	Flow gpm	T ₃ °C	0	1/2	1	1-1/2	2	2-1/2	3	3-1/2	4	4-1/2	5	5-1/2	6	6-1/2	7	7-1/2	8	8-1/2	9	9-1/2	
1.0	15.0	21.35	2.51	2.61	2.65	2.66	2.65	2.52	2.46	2.60	2.47	2.61	2.56	2.38	2.54	2.48	2.56	2.54	2.56	2.51	2.51	2.51	1.61
2.0	21.5	21.60	3.41	4.39	4.40	4.39	4.37	4.38	4.41	4.20	4.37	4.13	4.43	4.38	4.40	4.28	4.42	4.21	4.41	4.11	4.11	4.11	3.01
3.0	25.5	21.30	5.36	6.26	6.26	6.26	6.14	5.91	6.16	6.24	6.11	5.91	6.12	5.91	6.04	5.81	6.00	5.94	5.88	6.07	5.99	5.41	5.41
4.0	30.5	22.05	6.51	8.43	8.54	8.44	8.42	8.39	8.26	8.30	8.11	7.93	7.98	7.93	7.89	7.92	7.70	7.95	8.01	7.78	7.72	3.41	3.41
5.0	34.0	22.40	7.98	10.24	9.72	10.12	10.30	10.02	9.99	9.62	9.69	9.80	9.86	9.61	9.66	9.62	9.66	9.66	9.60	9.62	9.44	8.96	8.96
6.0	38.0	22.65	9.86	12.15	12.11	12.04	11.97	11.85	11.81	11.92	11.66	11.74	11.69	11.63	11.70	11.61	11.21	11.57	11.17	11.02	11.24	11.13	11.13
7.0	43.0	22.90	10.41	14.01	14.01	13.99	13.97	13.83	13.81	13.89	13.87	13.66	13.63	13.67	13.31	13.64	13.55	13.65	13.65	13.30	12.33	12.18	12.18

.065" WALL COPPER TUBE
 (SEAMLESS, DOUBLE PLENUM)
 CENTER FEED
 SLOT WIDTH: .063"

TABLE 2-11

P ₁ psi	Flow gpm	T ₃ °C	0	1/2	1	1-1/2	2	2-1/2	3	3-1/2	4	4-1/2	5	5-1/2	6	6-1/2	7	7-1/2	8	8-1/2	9	9-1/2	
0.5	9.0	19.50	1.13	1.15	.91	1.01	1.04	1.07	1.08	1.07	1.05	1.05	1.07	1.08	1.08	1.09	1.10	1.09	1.08	1.11	1.16	1.12	1.12
1.0	12.8	19.60	1.67	1.70	1.54	1.45	1.53	1.49	1.54	1.53	1.52	1.50	1.52	1.52	1.51	1.49	1.51	1.47	1.45	1.54	1.68	1.66	1.66

The bearing was a failure. Any movement of the film off-center in either direction was immediately magnified and caused an acceleration toward that end of the slot. At this point, the reason became obvious. A liquid bearing has an extremely low coefficient of friction (versus the high coefficient for the center of a crowned pulley wheel); consequently, a vector diagram quickly reveals the unstable nature of such a bearing. To duplicate the self-centering action of a crowned pulley, the pressure profile has to be high at the outer ends and lower in the center portion.

Such a bearing was quickly designed and built (Figures 2-18, 2-19, and Table 2-11). A double plenum and split center-feed obtained the desired pattern. A small pressure tap was added (after the film-support tests were completed) to the throat of the center-feed inlet pipe to determine the pressure drop in a large loop of rubber hose that was used to feed the bearing. These readings are included as "actuals." Certain imperfections in the execution of the bearing, resulting from the necessary haste with which it was assembled, prevented top performance, but the principle was confirmed.

Since center-feed offers numerous design, construction, assembly, operating, and maintenance problems in a typical processor, the next logical step was to duplicate the pressure profile with a single end-feed bearing. This was accomplished by tapering the slot from the center outward. From a 0.010-inch width on the center line, the slot was expanded to a maximum of 0.040 inch at the outer ends in the 4-3/4-inch distance. This was done by a series of step cuts on a logarithmic progression rather than a continuous taper because the shop could not machine a continuous taper at the time (Figure 2-20). Because of the peculiar construction of the bearing, it did not prove feasible to measure its pressure profile, but its performance was most encouraging. When film was manually moved as far as 5/8 inch off center and then released, it would immediately recenter itself and remain stable. At this point, all of the experimental findings could be incorporated into one design.



STAT

50087

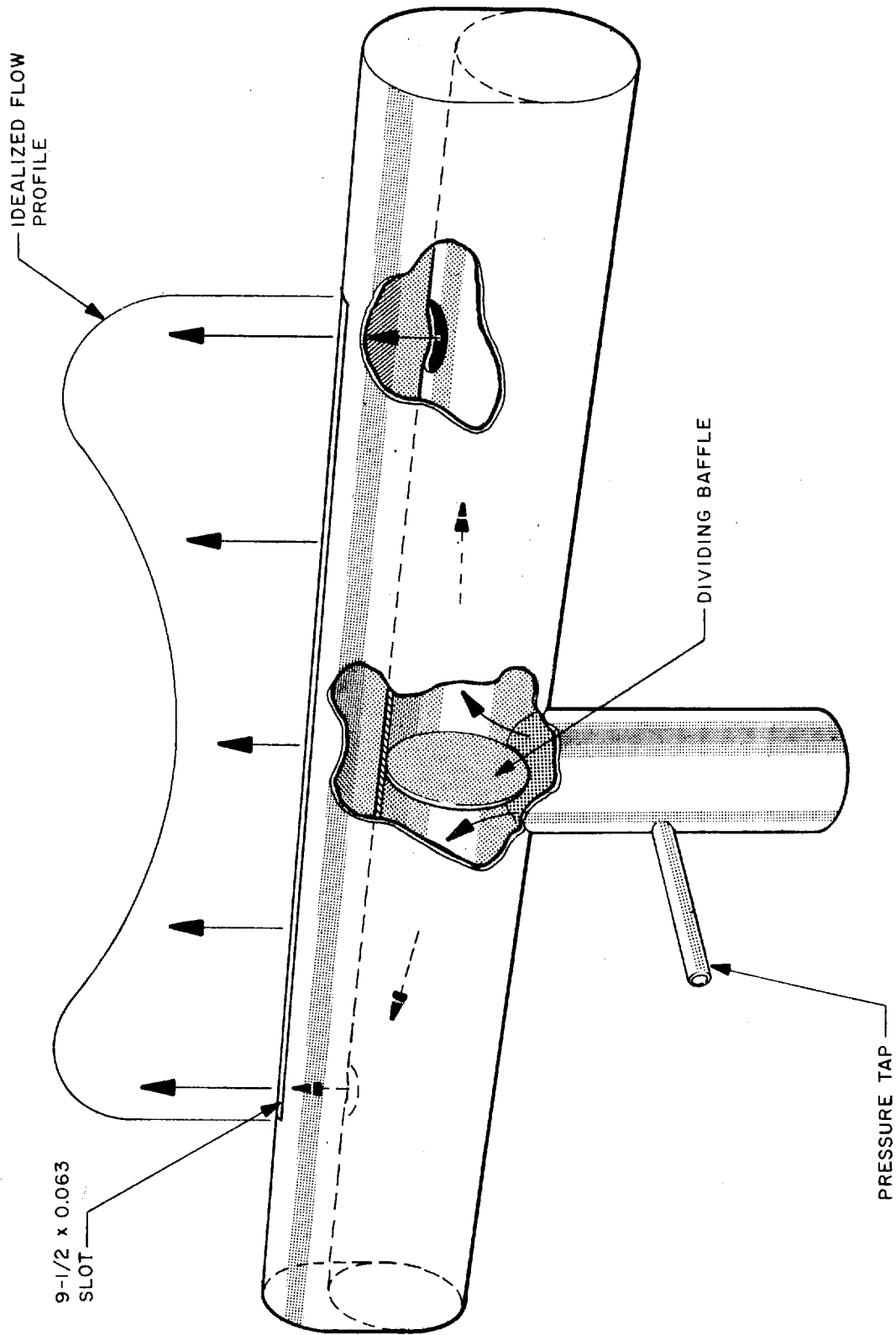


Figure 2-18. Double-Plenum Center-Feed Copper Bearing

50088

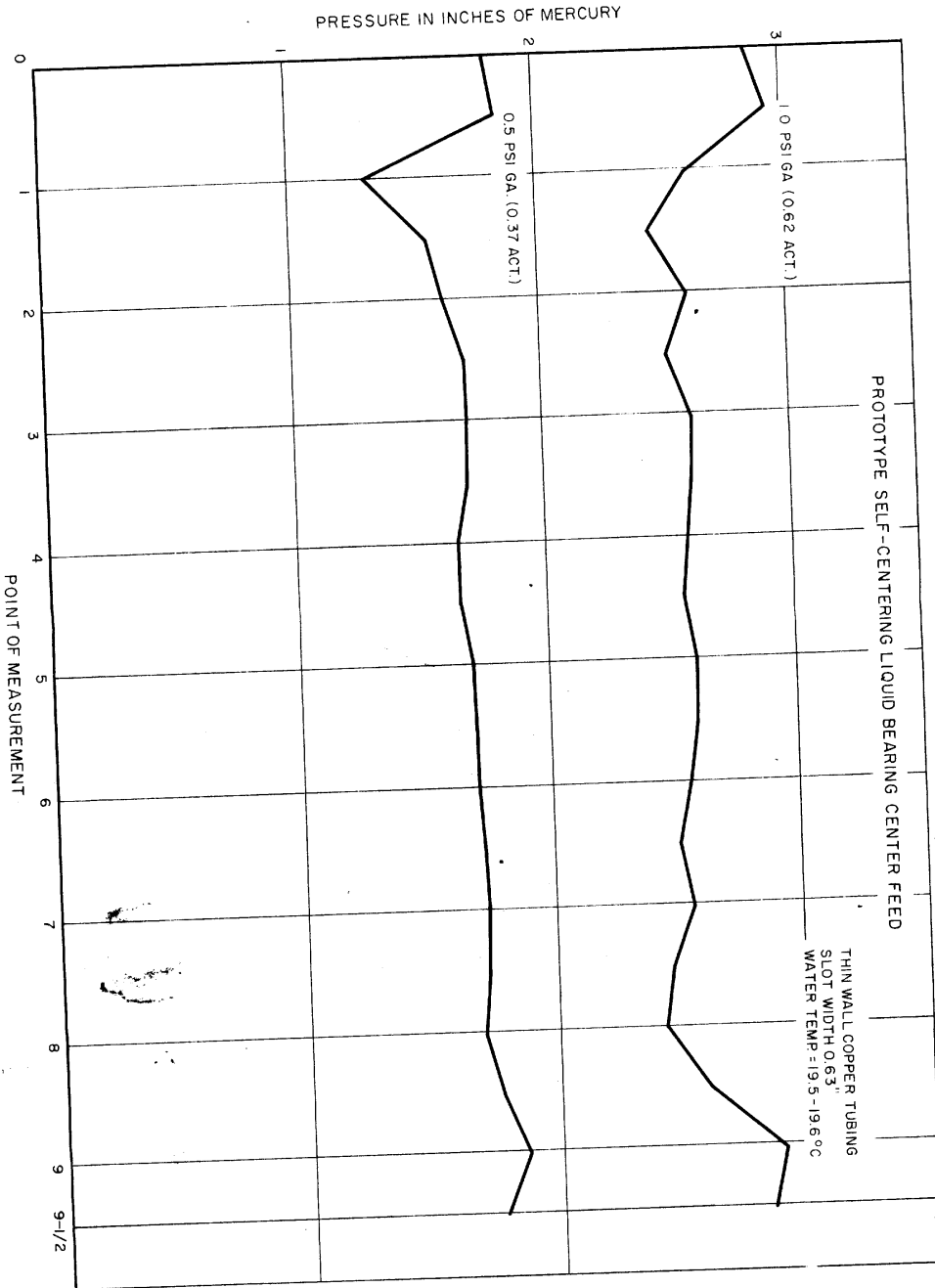


Figure 2-19. Pressure Profile of Center-Feed Copper Bearing

STAT

2-32

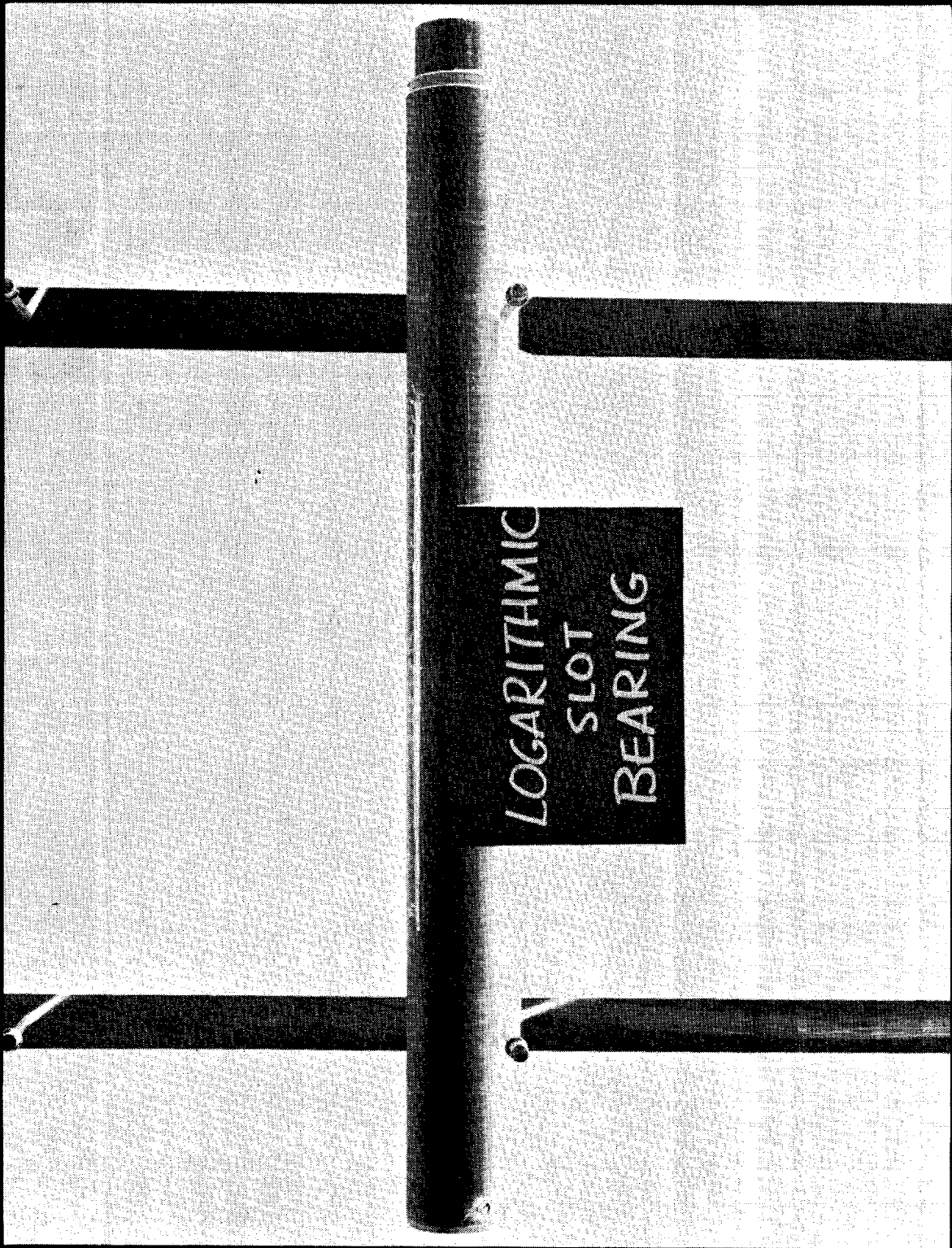


Figure 2-20. Logarithmic Slot Self-Centering Liquid Bearing

2.2.4 Methacrylate End-Feed Self-Centering Liquid Bearing

The bearing was built of clear methyl methacrylate tubing, cast and polished, having an outside diameter of 2-1/2 inches and an inside diameter of 2 inches (Figures 2-21 and 2-22). The outside of the tubing was tapered 1/8 inch in 5 inches toward the center over the area on which the film rides. The tubing was then split in half lengthwise and three slots were milled in one of the halves. The top slot was tapered from 0.008 inch (at the center) to 0.025 inch in 4-3/4 inches. The two side slots were each 0.020 inch, untapered. As illustrated, one was tipped to lead the film and the other to follow it slightly (rather than being machined on a radius line) to prevent cushion collapse under load. After milling, the inside edges of each slot were faired to reduce turbulence and coefficients of friction.

Since two of the slots were near the edge, and the plastic is inherently quite weak, the whole half-bearing was supported in a plaster of paris matrix for the machining operation. After machining, the bearing was assembled with an internal feed pipe in the same manner as previous metal models.

When first tested with the film supporting a total dry weight of 519.2 grams, a 1/4-inch cushion with an inlet pressure of 0.5 psi and a flow of 13 gpm was attained. However, the film tracking was not stable and tended to drift off on either side of the slots. Since the prototypes had been successful, a pressure traverse of the three slots was made. This confirmed the hypothesis that the side slots (combined area of 0.380 square inches) were overriding the beneficial self-aligning effect of the main slot (area of 0.157 square inches).

(Continued page 2-37)

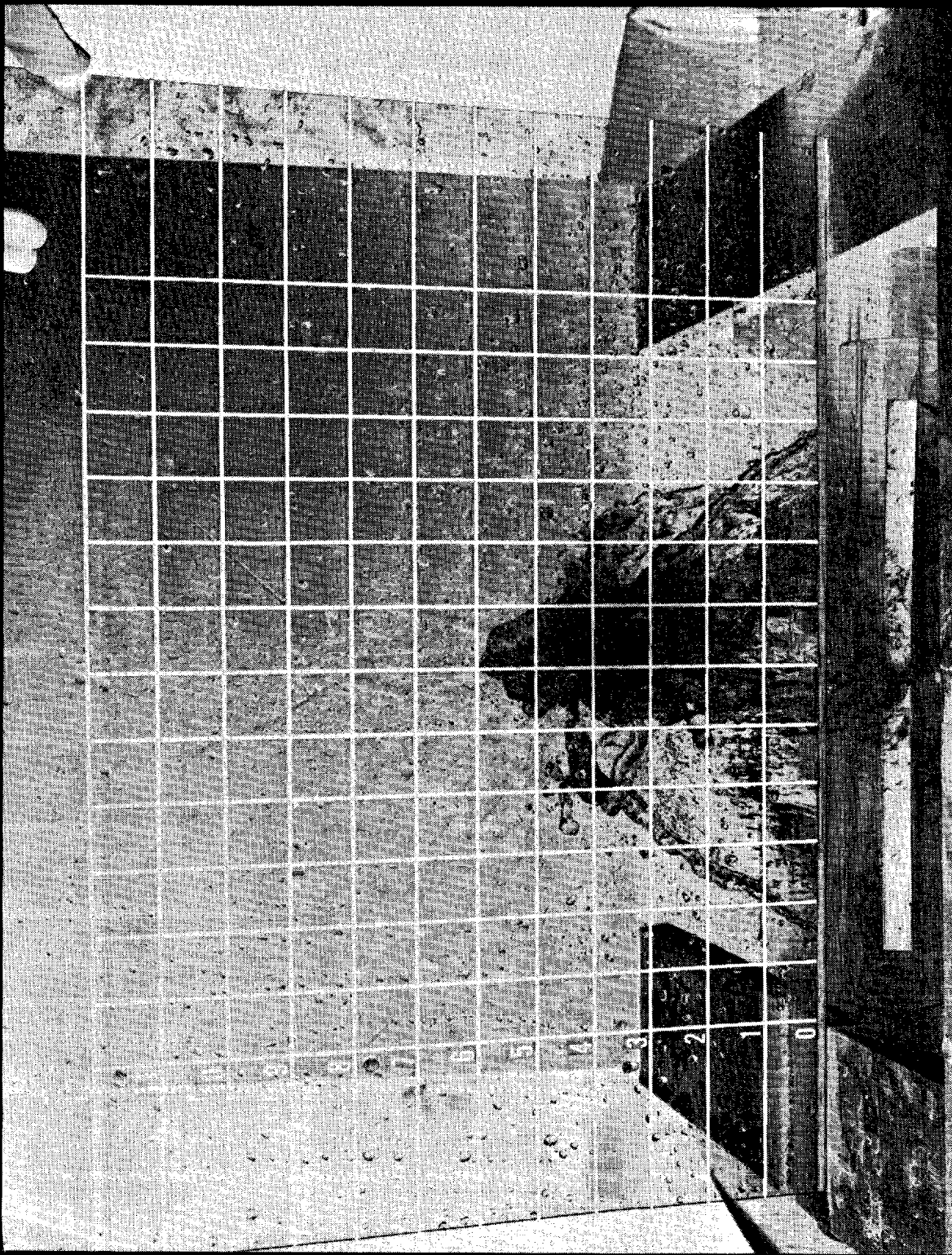


Figure 2-21. Methacrylate Self-Centering Bearing

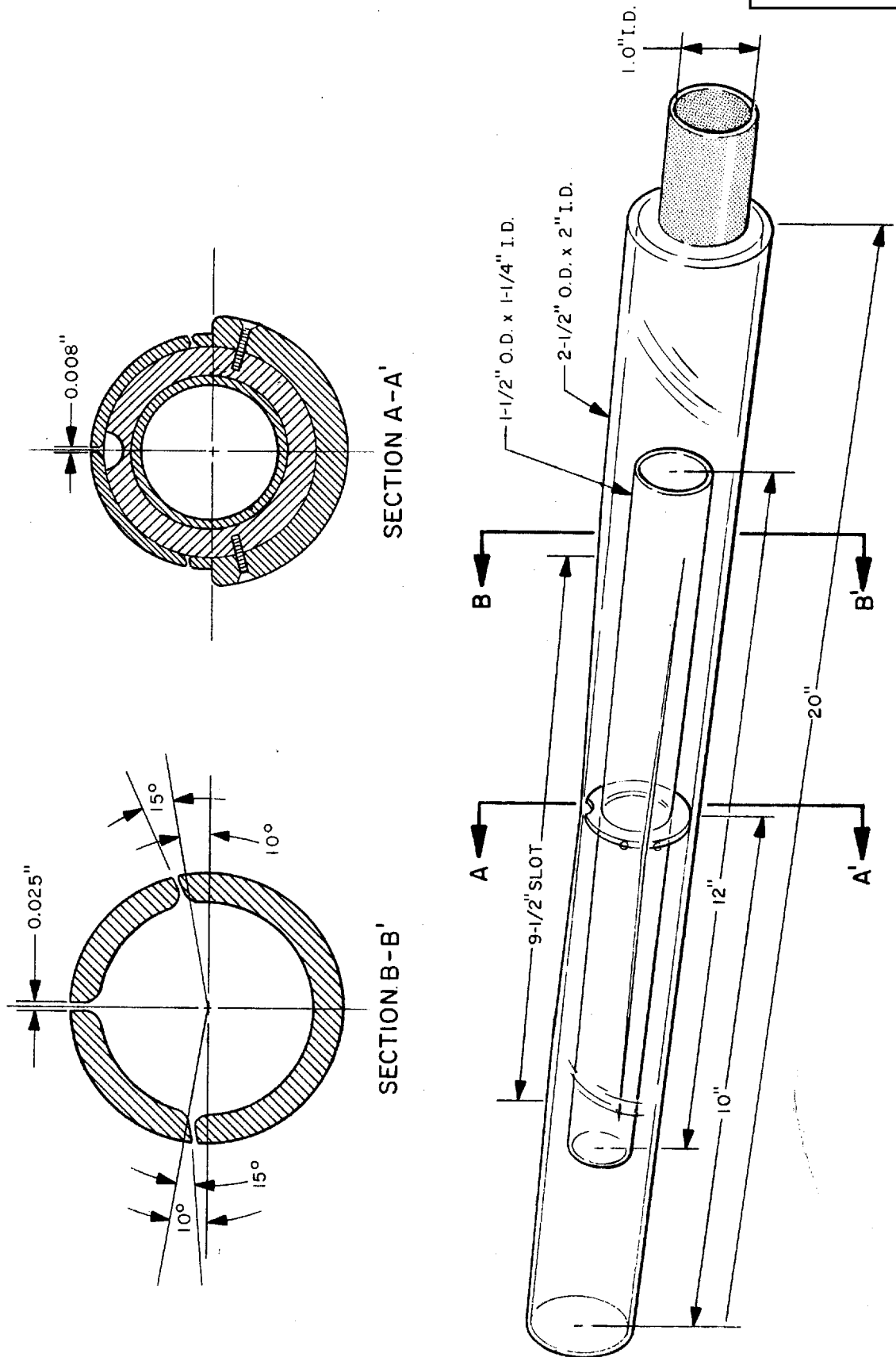


Figure 2-22. Cutaway Showing Construction of Methacrylate Tapered-Slot, Self-Centering Bearing

Four knife blades were constructed of 0.016 inch stainless steel shim stock and affixed to the periphery of the upper portion of the bearing so as to taper the side slots from a maximum of 0.020 inch at the outer ends to a minimum of 0.005 inch at the center. When retested with a continuous film loop supporting a spool (dry weight 354.5 grams), the bearing was self-centering. At an inlet pressure of 0.6 psi and a flow of 17 gpm, the cushion was fairly stable but there was some hunting as the film tracked. This may have been due to slight fluctuations in the line pressure introduced by the centrifugal pump. However, when pulled as far off center as 1-1/2 inches, the film would immediately move back to the center line.

The original 354.5-gram spool used had a 1.30-inch diameter spindle. This relatively narrow width allowed the adjacent sides of the film to cohere, somewhat, because of the Bernoulli effect introduced by the fast flow from the side slots in the confined area within the film loop. When this effect was minimized by the introduction of a heavier spool (four pounds dry weight) of larger spindle diameter (3.50 inches), a truer measurement could be made. The new bearing, at an inlet pressure of 0.4 psi and a flow of 10.5 gpm duplicated the lifting capacity (3/16-inch stable cushion) of its forerunner, the standard HTA-5 bearing, at a pressure of 1.5 psi and a flow of 26 gpm. When these figures are translated into horsepower, the requirement of the new design is approximately 1/10th that of the old. With the heavier load, however, the self-centering tendency was not as pronounced unless the film was spun over the bearing.

Because of the thickness of the stainless shims (0.016 inch) used to create the taper, some distortion in the cushion profile resulted from water flowing over the obstruction. It was felt that this also was adversely affecting the self-centering feature. As a consequence, the bearing was disassembled and modified by the addition of plastic to conform closer to

its original design parameters. All subsequent testing was performed on this modified version of the bearing.

In the first series of tests, the weight lifting capability of the tapered bearing was assessed by applying successive loading to a spool supported by a loop of 9-1/2-inch medium-base, black aero leader. The weights were varied from 1 pound through 7 pounds in 1-pound increments. Although the bearing showed ample evidence of being capable of sustaining heavier loads, 7 pounds was selected as a reasonable cut-off point since it is greater than the maximum operating single-bearing load in any liquid bearing processor hither to designed and built [REDACTED] STATINTL

The results are tabulated (Table 2-12) and graphed (Figures 2-23, 2-24, and 2-25). Reference to column B of Table 2-12 shows the cushion height on the top of the bearing constant at 0.016 inches for loadings of 1 pound through 5 pounds and a flow of 13.5 gallons per minute. This phenomenon (Curve B, Figure 2-24) has interesting ramifications. If, for this type of bearing design, the cushion height is relatively independent of load at constant flow, it suggests that a series of such bearings would not require feed-back mechanisms, or throttling devices to compensate for the progressive loading of the bearings from film entrance to exist in the processor. In other words, there is a strong possibility that such bearings might prove self-adjusting for load. This theory would have to be checked on a full scale mockup as it cannot be predicated mathematically nor safely based on the empirical results of testing one unit only.

Figure 2-24 also shows another characteristic. As loading increases, the leading- and trailing-edge cushions are compressed as would be expected. However, at 6 and 7 pounds, the center cushion (at point B) actually increases. Thus, it would appear to have a built-in safety factor which would prevent functional film damage at high loading levels.

(Continued page 2-43)

TABLE 2-12
 ANNULAR VELOCITY, CUSHION HEIGHT, SUPPORTED WEIGHT
 (9-1/2-Inch Aerial Film, Medium-Base, Black Leader)

Wet Weight Pounds	Film Loading psi	Flow gpm	Pressure psi	Temp °F	A Inches	B Inches	C	Annular Area In ²	Transverse Area In ²	Velocity fpm
1	.024	13.5	0.8	72.52	.062	.016	.250	2.046	2.983	0.81
2	.050	13.5	0.8	72.78	.055	.016	.156	1.260	1.278	1.61
3	.077	13.5	1.0	72.25	.031	.016	.101	.778	1.250	2.01
4	.105	13.5	1.0	72.12	.016	.016	.047	.347	.597	4.32
5	.131	13.5	1.0	71.72	.016	.016	.043	.316	.559	4.66
6	.158	13.5	1.1	71.23	.016	.023	.039	.437	.521	4.25
7	.185	13.4	1.1	70.86	.016	.047	.031	.453	.445	4.54

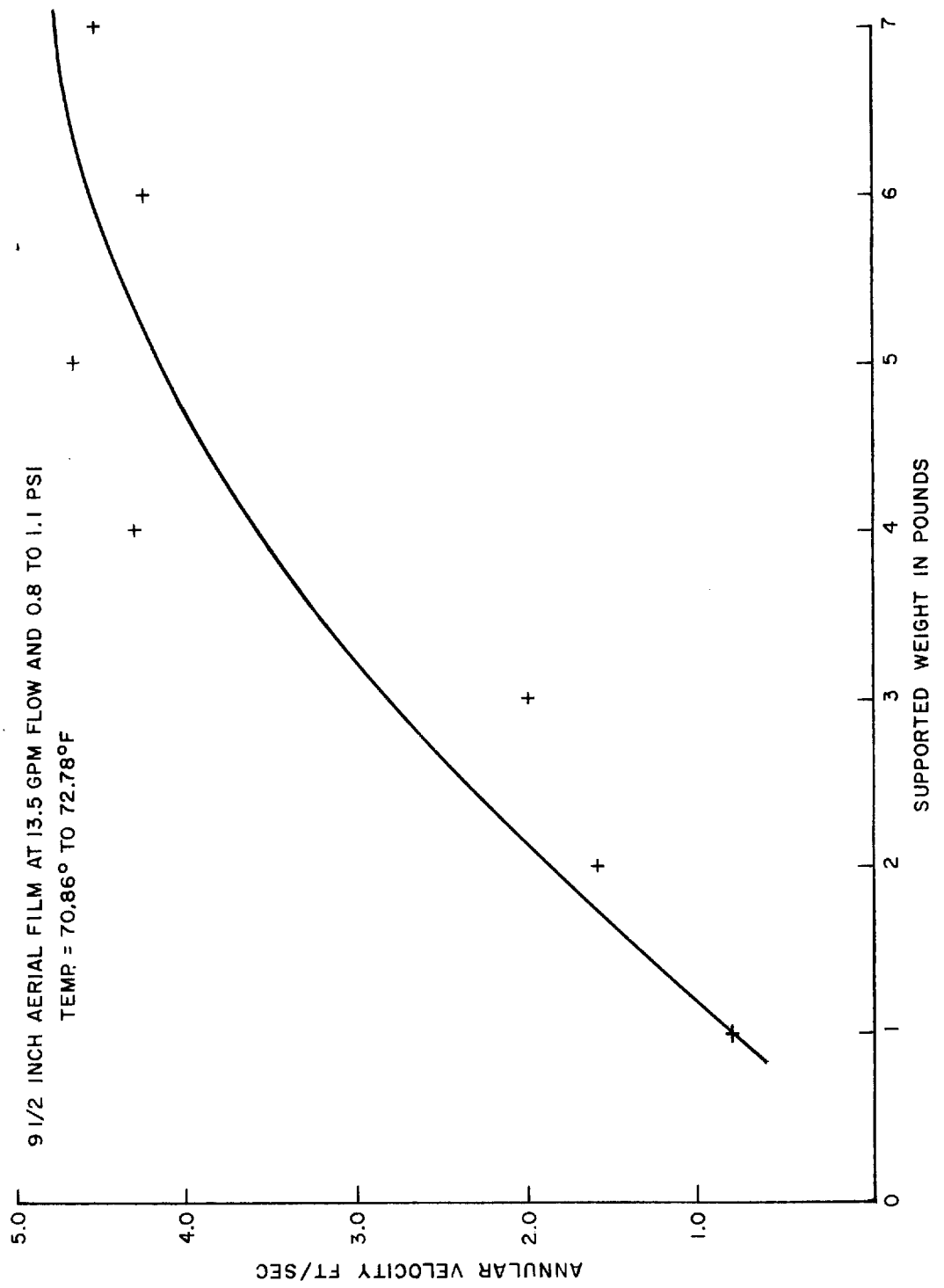


Figure 2-23. Annular Velocity Versus Supported Weight - 9-1/2 Inch Film

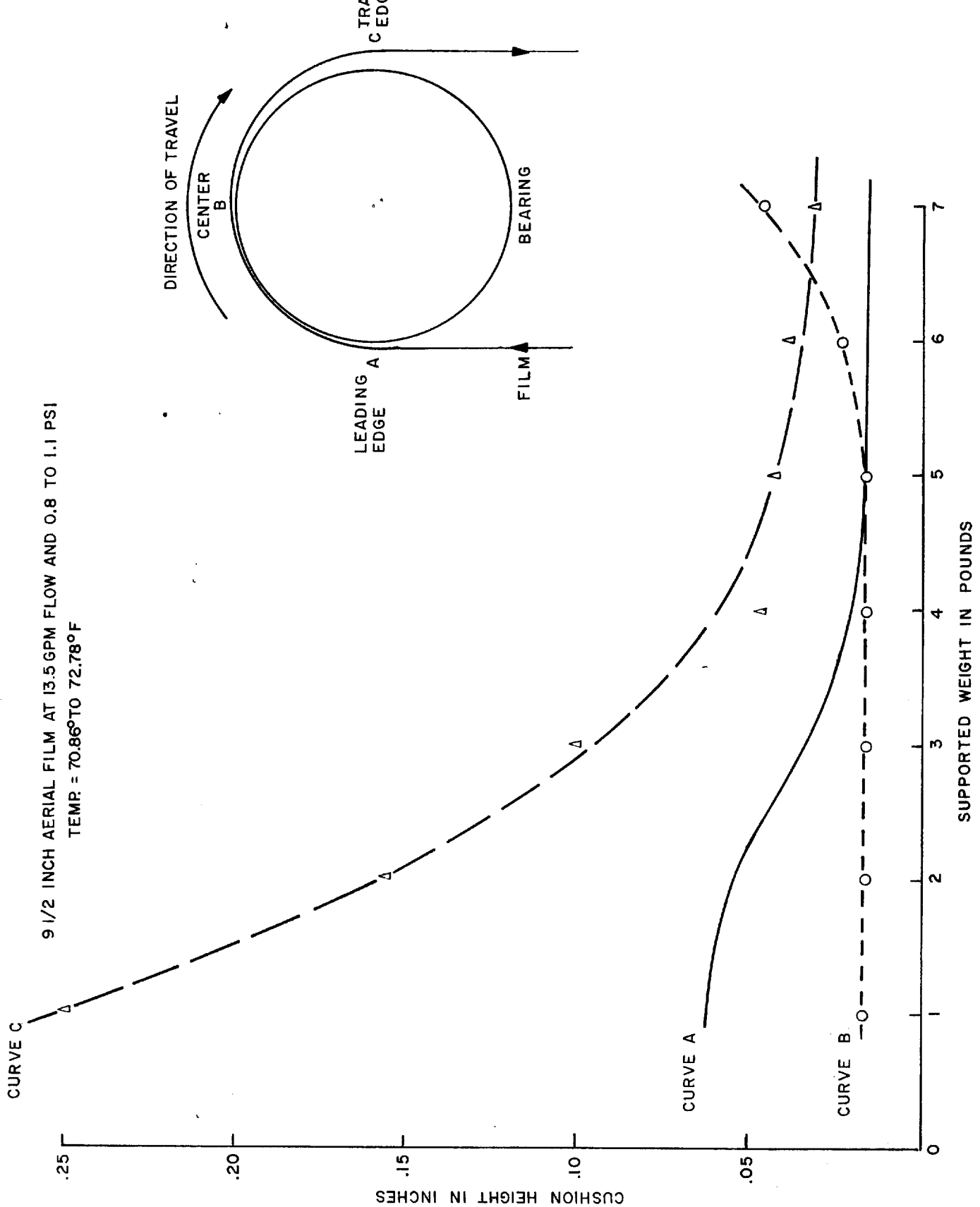


Figure 2-24. Cushion Height at Constant Flow and Varying Weight - 9-1/2-Inch Film

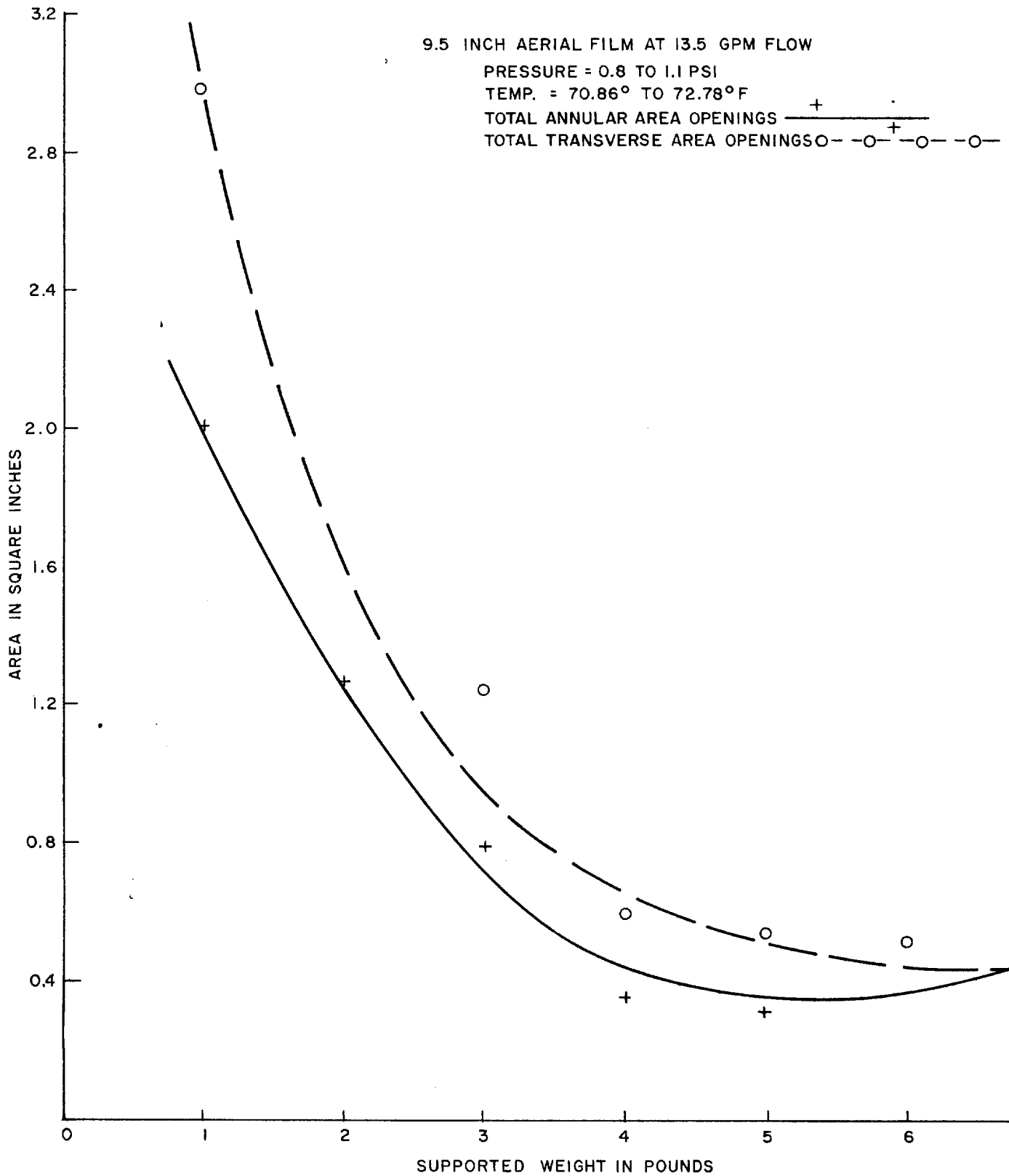


Figure 2-25. Annular and Transverse Areas at Different Weight Loadings - 9-1/2-Inch Film
Approved For Release 2002/09/03 : CIA-RDP78B04747A002800010001-0

Whether or not the reaction time would be fast enough to prevent the film from suddenly being forced down on the crown of the bearing if the load were applied instantaneously, would have to be carefully checked experimentally. At any rate, former liquid bearing designs did not exhibit this propensity.

Because of the way in which the measurements were made, it was possible to calculate both the annular area of liquid escape at the sides of the film and the transverse area at the leading and trailing edges of the bearing. A plot (see Figure 2-25) shows the inter-relationship of these areas. As loading was increased, they approached the same value and their ratio becomes unity at 7 pounds. The areas were totalled for each load and the escapement velocities calculated. This plot appears in Figure 2-23.

One of the most interesting observed characteristics of the bearing proved to be the following. The film reel and lead weights used to create the different loading values did not permit the reel to spin. A special reel, having a wet weight of 3 pounds, was prepared so that it could spin freely in the film loop. When this reel was in place and the bearing activated, the film loop would revolve at about 12 feet per minute. Thus, rotary power was being imparted to the film at the same time as cushion support was provided. Since rotation indicates that the forces of drag, film weight, and bend radii have been compensated, it can be premised that a series of such bearings would not place a torque load on the drive capstan. This effect might prove to be a mixed blessing, however, since some loading is necessary to provide stable tracking. In such instance, sufficient artificial drag would have to be introduced to assure proper tracking.

The self-centering design parameter was greatly enhanced by the modification, being capable of returning the film to center when pulled off as much as 3 inches. The film would also return when the bearing was tipped as much as 1/16-inch off level. However, the action was not as rapid as could be desired and the film would invariably overtravel before stabilizing at the center. The action was much faster in the case of the rotating loop and it can safely be surmised that a series of such bearings, with the film moving, would be more stable than the single unit.

A new series of static pressures was taken (Figure 2-26 and Table 2-13) with the improved pitot probe. The profiles for slots A and B, Figure 2-26, show how closely these approach the theoretical design ideal. Plot C, however, does not dip sufficiently at the center to provide adequate centering tendencies. To find out why this occurred, width readings (with a feeler gage) were taken along each slot at the same 1/2-inch intervals used for the pressure measurements. The results are tabulated (Table 2-15). It can be seen how closely the pattern follows the actual slot width by comparing these figures with the graph (Figure 2-26). This test underlines the importance of meticulous care in manufacturing this type of bearing and the use of a plastic material not as subject to deformation as methacrylate. It is felt that if the trailing-edge slot were corrected to theoretical taper, the self-centering feature would be improved proportionately.

The foregoing series of tests was followed by measurements to determine how well the bearing could support narrower widths of film without slot format changes. The results were disappointing. With flows as high as 20 gpm at 3 psi, 70mm film supporting a weight of 1-3/4 pounds (approximately 0.139 pounds per square inch of supported film) showed a cushion of only 1 mil. While the self-centering was immediate, this low cushion does not afford a sufficient safety factor. With a flow of 17.5 gpm at 2 psi, 6.6-inch film could be supported on a 2-mil cushion, but the

(Continued page 2-48)

STAT

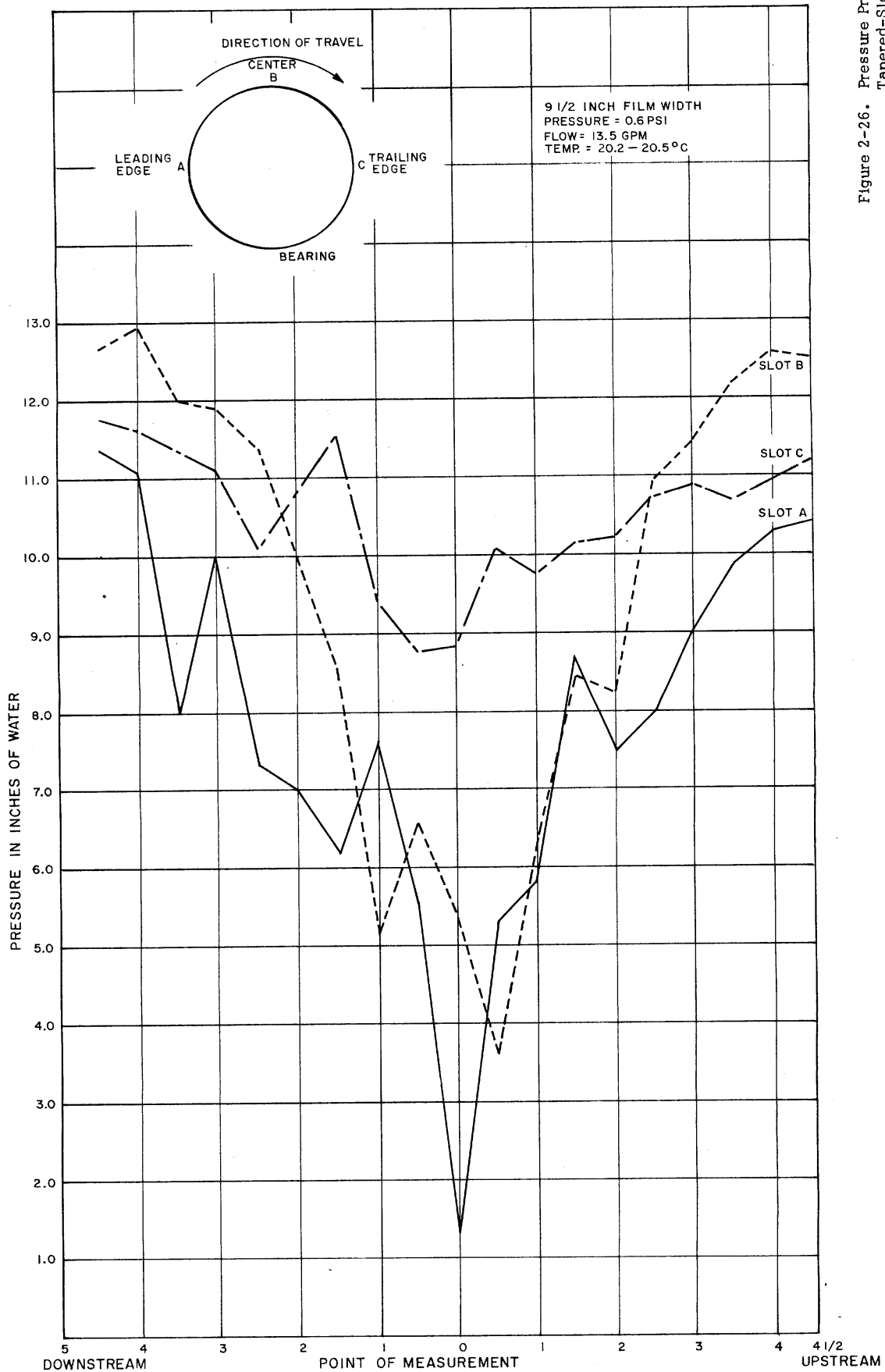


Figure 2-26. Pressure Profile for Tapered-Slot Liquid Bearing 9-1/2-Inch Width

STAT

TABLE 2-13 -- PRESSURE PROFILE MEASUREMENT DATA FOR TAPERED-SLOT LIQUID BEARING (9-1/2-Inch Width)

Pressure psi	Flow gpm	Temp °C	Downstream				Upstream														
			4-1/2	4	3-1/2	3	2-1/2	2	1-1/2	1	1/2	0									
A	13.5	20.4	11.35	11.05	7.97	9.94	7.32	6.98	6.18	7.64	5.55	1.38	5.27	5.79	8.68	7.44	8.43	9.02	9.85	10.27	10.40
B	13.5	20.2	12.63	12.90	11.98	11.85	11.35	10.00	8.50	5.13	6.58	5.35	3.62	6.25	8.43	8.24	10.92	11.44	12.17	12.57	12.50
C	13.5	20.5	11.72	11.58	11.32	11.05	10.07	10.80	11.52	9.42	8.75	8.82	10.07	9.74	10.14	10.20	10.72	10.86	10.67	10.93	11.19

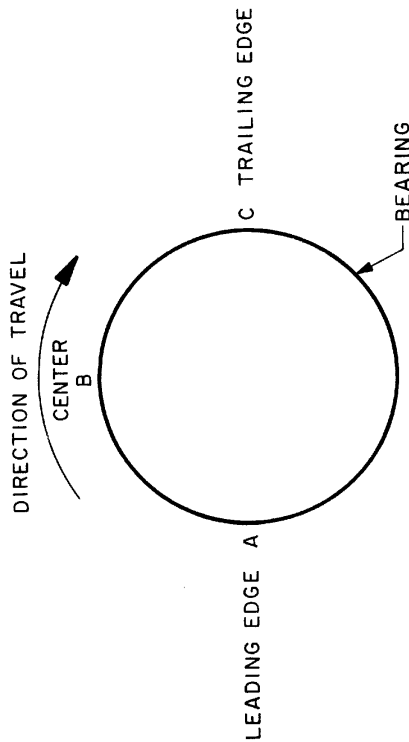
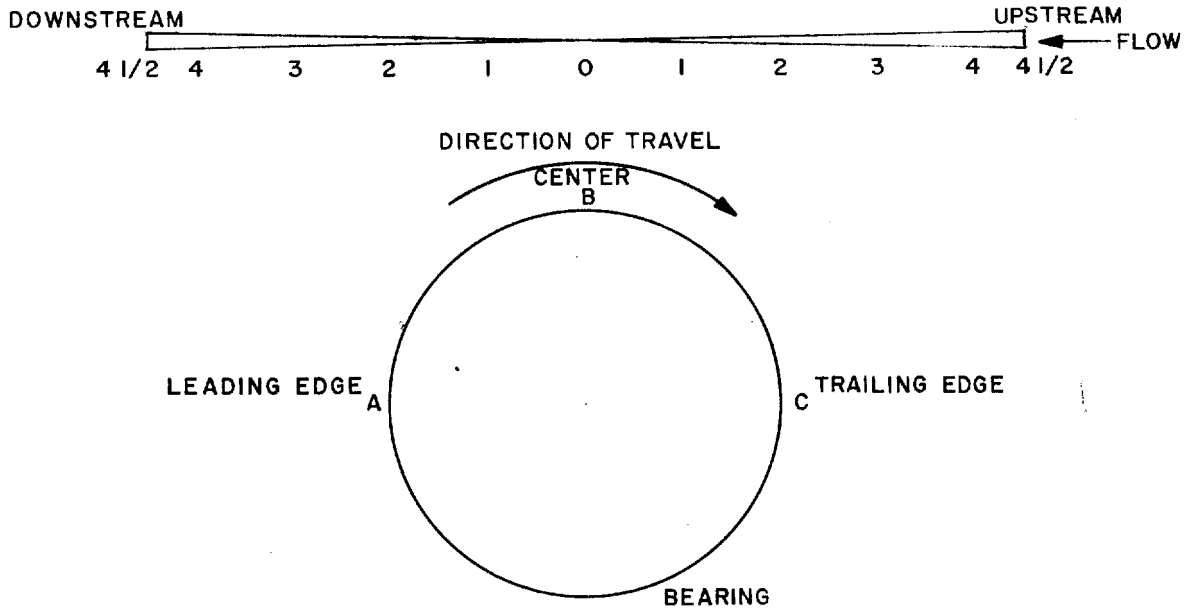


TABLE 2-14 -- PRESSURE PROFILE MEASUREMENT DATA FOR TAPERED-SLOT LIQUID BEARING (6.6-Inch Width)

Pressure psi	Flow gpm	Temp °C	Downstream			Upstream									
			3	2-1/2	2	1-1/2	1	1/2	0						
A	13.0	19.8	24.40	23.05	26.50	21.20	22.00	9.35	6.58	16.60	16.80	22.60	22.00	26.80	25.20
B	13.0	18.2	29.30	29.60	27.90	26.10	24.90	21.50	10.80	13.75	19.74	23.90	27.40	28.40	29.80
C	13.4	19.4	28.50	27.90	27.70	28.80	24.10	27.10	22.20	27.10	27.00	28.40	29.70	27.70	28.90

TABLE 2-15
BEARING SLOT WIDTHS

TAPERED SLOTS



		in 1/1000's Inch		
Point of Measurement		A	B	C
Downstream	4-1/2	20	23	21
	4	18	22	19
	3-1/2	16	20	16
	3	14	18	16
	2-1/2	12	16	16
	2	11	13	16
	1-1/2	10	10	16
	1	10	9	16
	1/2	7	8	15
	0	6	8	15
	1/2	8	8	16
	1	10	9	16
	1-1/2	11	12	17
	2	14	15	17
	2-1/2	16	17	18
	Upstream	3	18	20
3-1/2		18	22	20
4		18	25	21
4-1/2		20	25	25

inherent advantage of low power consumption was, of course, lost. Once it had been proved that format changes were a necessity, the tests were repeated on 6.6-inch film after the slots had been masked down to film width by strips of mylar splicing tape. These tests are summarized in Figures 2-27, 2-28, 2-29, and 2-30, and Tables 2-14 and 2-16.

The tests, for the most part, duplicate fairly closely the findings for the 9-1/2 inch film width. Some points are, however, worthy of note. The pressure profile shows approximately double the values obtained for the wider film at comparable loadings. Secondly, the cushion was far less stable at light loads, and, for the lowest readings, the flow had to be reduced in order to get significant values. Lastly, the velocity plot (Figure 2-27) did not flatten out at higher loadings but continued to a maximum. All of these factors point to lower efficiency and suggest that for this type of bearing, the ideal design would match the bearing to each film width.

The bearing is an improvement in many ways over previous liquid bearing designs in the parameters examined. It did not, however, fulfill all the objectives of the program. The tests are incomplete in so far as nothing is known about its effect on film when used with actual photographic chemicals, and the effect on performance, if the format change feature is added, cannot be predicted.

(Continued on page 3-1)

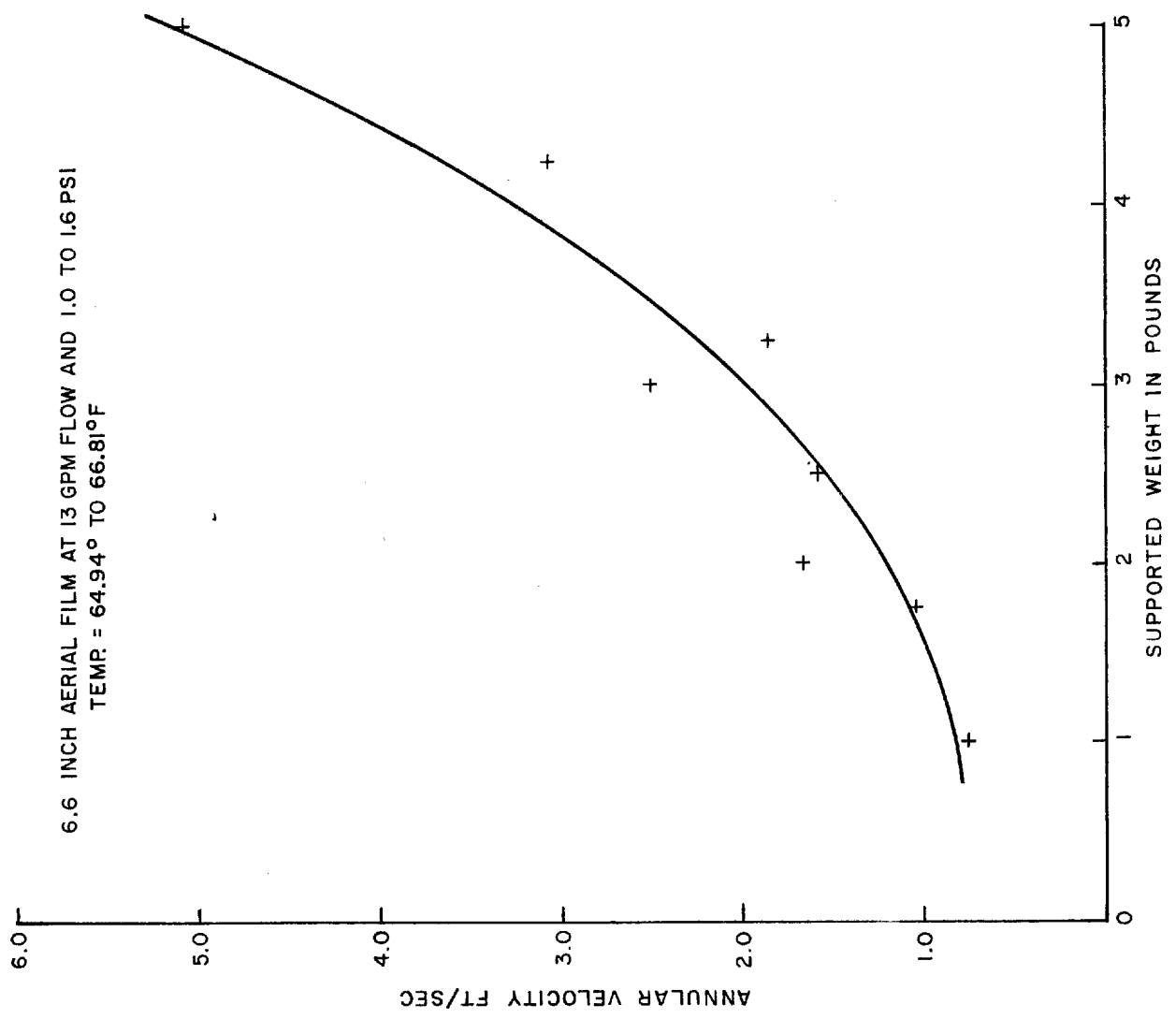


Figure 2-27. Annular Velocity Versus Supported Weight - 6.6-Inch Film

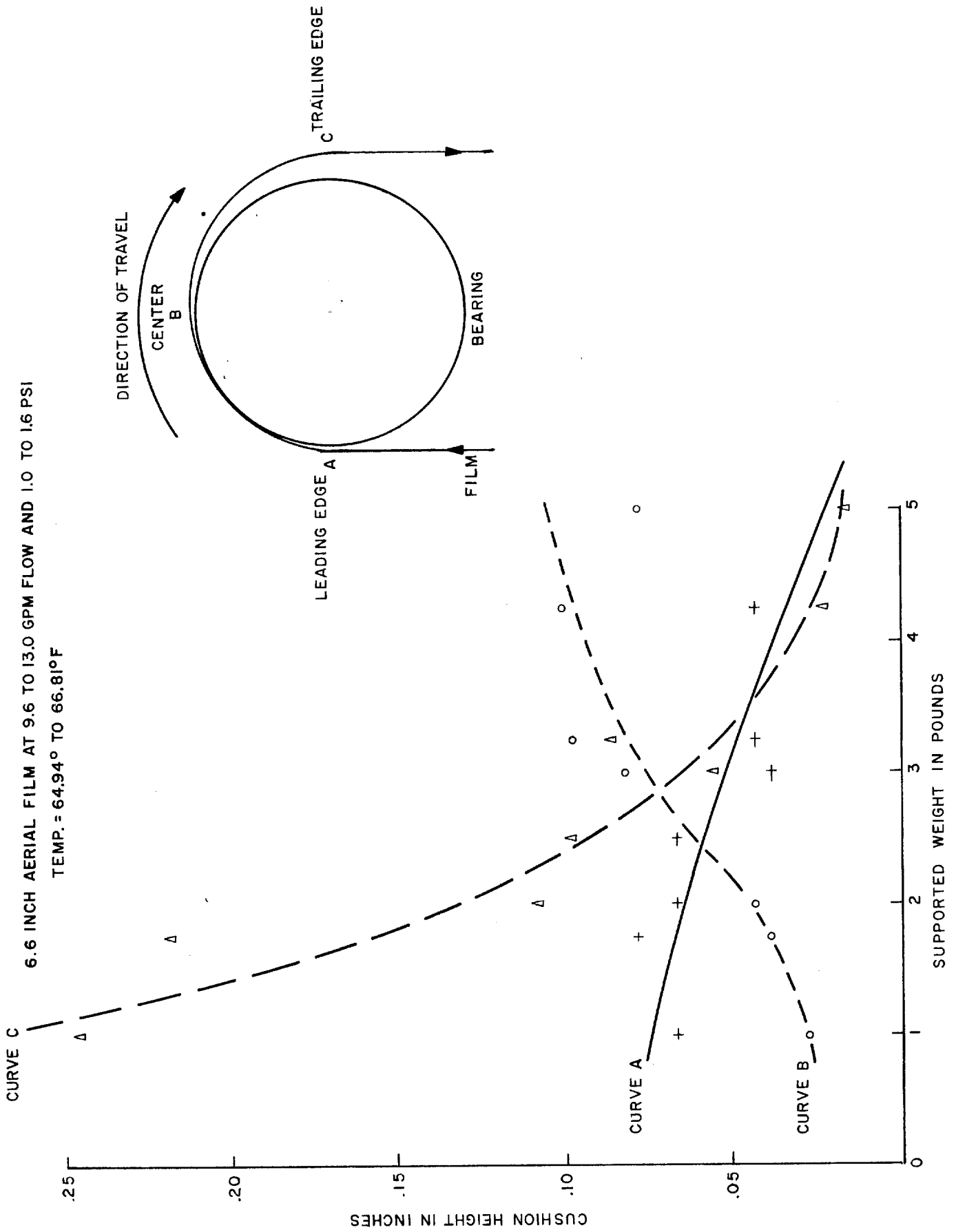


Figure 2-28. Cushion Height at Constant Flow and Varying Weight - 6.6-Inch Film

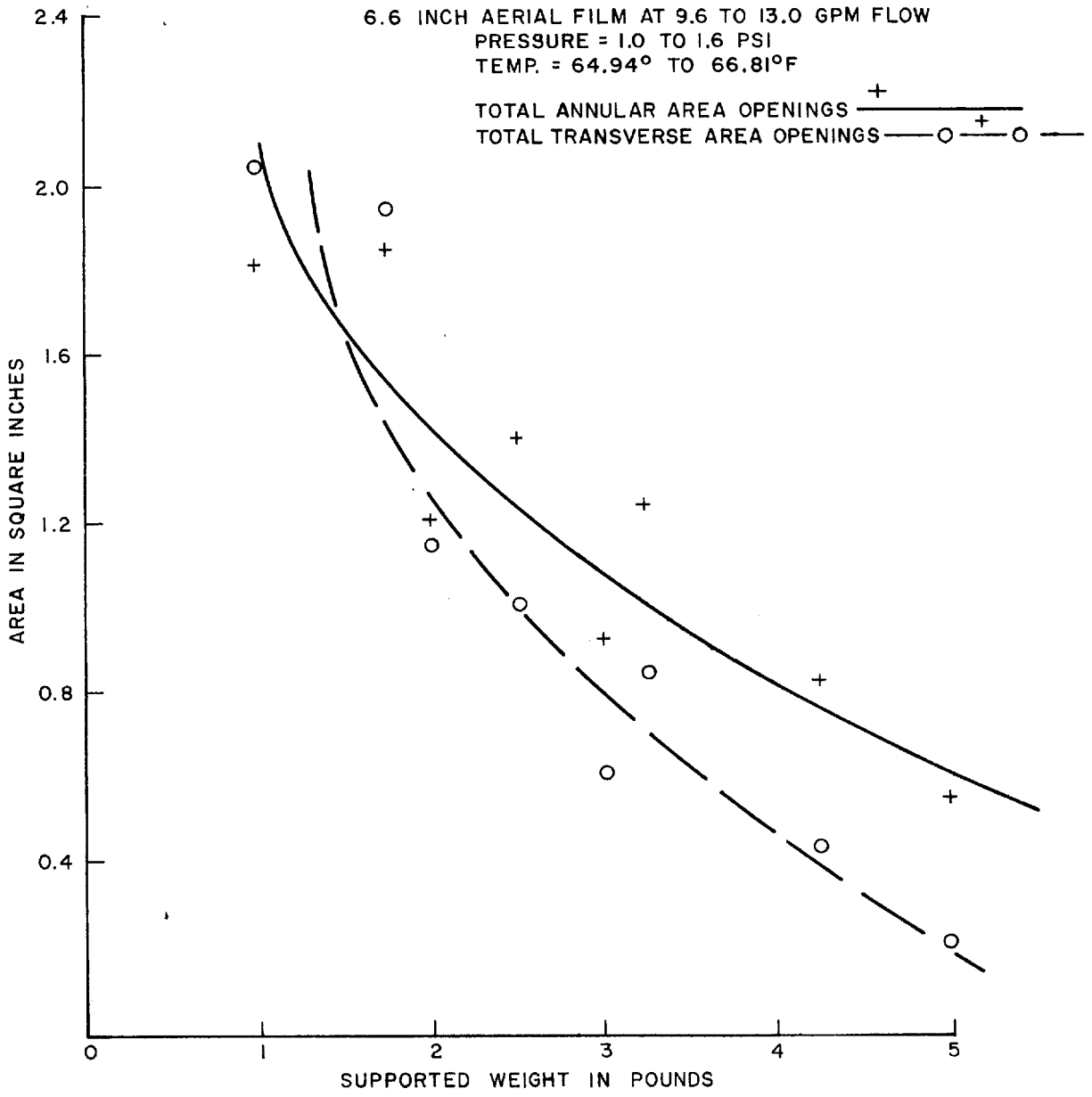


Figure 2-29. Annular and Transverse Areas at Different Weight Loadings - 6.6-Inch Film

STAT

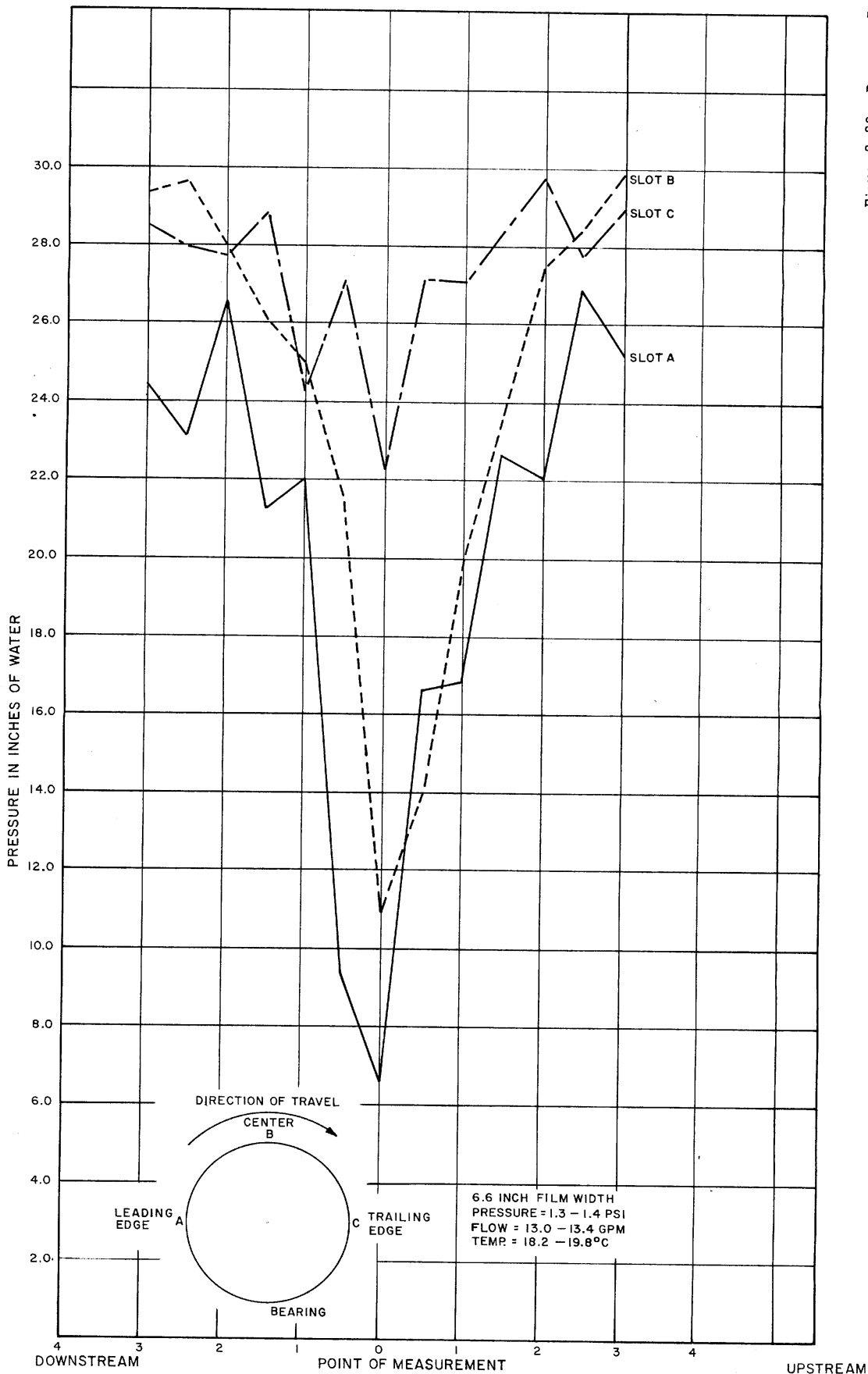


Figure 2-30. Pressure Profile for Tapered-Slot Liquid Bearing, 6.6-Inch Width

TABLE 2-16
ANNULAR VELOCITY, CUSHION HEIGHT, SUPPORTED WEIGHT
(6.6-Inch Special Fine Grain Aerial Duplicating Safety Film)

Wet Weight Pounds	Film Loading psi	Flow gpm	Pressure psi	Temp °F	A Inches	B Inches	C	Annular Area In ²	Transverse Area In ²	Velocity fpm
1	0.034	9.6	1.0	65.12	.066	.027	.246	1.816	2.059	0.73
1-3/4	0.060	13.0	1.5	66.81	.078	.039	.218	1.848	1.954	1.02
2	0.072	13.0	1.5	65.00	.066	.043	.109	1.208	1.155	1.64
2-1/2	0.091	13.0	1.5	65.15	.066	.098	.098	1.396	1.082	1.57
3	0.111	13.0	1.5	65.15	.039	.082	.055	0.934	0.620	2.50
3-1/4	0.119	13.0	1.5	65.20	.043	.098	.086	1.250	0.852	1.85
4-1/4	0.160	13.0	1.5	64.94	.043	.101	.023	0.834	0.436	3.06
5	0.190	13.0	1.6	65.12	.016	.078	.016	0.556	0.211	5.06

SECTION 3
SUMMATION OF FINDINGS

3.1 NARROW LIQUID BEARINGS

Narrow liquid bearings, while economic from the standpoint of pressure and flow required to lift a specified load, had two serious limitations. The first was the difficulty of producing a desired pressure profile by means of internal wedge shaped equalizers or other devices. The second was the fact that they would only be practical for extremely thin film and leader where the bending force required to conform to the small radius was negligible compared to the lifting force.

In narrow end-feed bearings in which the internal diameter was in the order of 1/10th the total bearing length, the pressure profile produced was parabolic in shape, with the high pressure point downstream from the feed. From this series of test results, the following hypothesis was formulated.

Liquid bearings having an identical cross-sectional configuration and area will produce a characteristic pressure profile plot whose magnitude at constant inlet pressure is directly proportional to flow.

3.2 END-FEED LIQUID BEARINGS

Single-slot, end-feed liquid bearings without provision for internal equalizing were impractical as film-supporting units for two reasons. In cross-section, the highest point of the cushion was at the top center and, from this point, it fell off rapidly on either side, virtually to zero at the 180-degree line (X-axis). The parabolic pressure pattern described earlier caused the film to tilt and move off the supporting slot. The skewed angle made accurate measurement of the cushion impossible.

When these empirical data were compared on a single graph (Figure 2-16), the significance of the construction material, the machine finish of the slot, the smoothness of the internal surface of the tubing, and the position of the seam relative to the slot became apparent. These represent the critical performance parameters.

3.3 SELF-CENTERING LIQUID BEARINGS

A new principle of equalizing the flow pattern in a single-slot liquid bearing was developed. A concentric inner tube supported by a center bulkhead produced a symmetrical pattern. When this pattern was modified to a "bow-tie" pressure profile (high at the outer ends of the slot and lower in the center), the film exhibited self-centering tendencies.

All of the experimental findings were incorporated in a single bearing made of methacrylate. This unit proved to have an outstanding performance capability at modest flow rates and inlet pressures. Its power requirements for equal work loads were approximately 1/10th that of the old standard HTA-5 bearing. Furthermore, at certain load-pressure balances, it tended to advance the film automatically.

The methacrylate bearing fell short of design expectations in that it required format changes for different widths of film and its efficiency dropped for narrower widths. On the plus side of the ledger, however, it showed evidence of being self-adjusting to increased loading at constant flow.

3.3.1 Liquid Bearing Design Procedure

1) Calculate maximum bearing load. [] details the step-by-step procedure by which desired film parameters and operating speeds of a hypothetical processor are converted into individual bearing loading. The methodical handling of the three factors contributing to

STAT

load (film drag coefficients, wet weight of film, and bend radii forces) give an accurate prediction of the maximum bearing load for the last liquid bearing in the wet end of the processor. Start by making this calculation for the widest film the processor is expected to handle. Assume heavy-base leader for purposes of calculation as this represents the heaviest load condition.

2) Select bearing size. The data presented in Figure 2-16 suggests that the lower limit of bearing inside diameter is 1-1/2 inches before distortion of flow pattern is the controlling factor. The upper limit depends upon two parameters: overall processor size and total horsepower considerations. To determine optimum size, make a twice-scale (or more) drawing of the proposed bearing. Use the outside diameter since this controls the bend radius. Select appropriate cushion heights from Figure 2-24 or 2-28 at the calculated loading and lay these in. Draw a circle through these three points and calculate the value of 1/2 of its circumference. This figure times the width of the film gives the total square inches of film acted upon by the liquid cushion.¹ Determine the loading in pounds per square inch. (The maximum tested in this assignment was 0.185 psi.) If the loading exceeds 0.185, select a larger diameter bearing and repeat the calculation.

3) Determine number of slots required. A single slot does not provide sufficient side cushions for a circular cross-section to overcome the Bernoulli effect inherent in the moving film sheath. The minimum number of slots which will assure even wetting of the film is the ideal. There are two practical limitations to be considered:

¹ Integration of the hydraulic forces acting on the film shows that not all are contributing to lift, but, for this approximation, the whole wetted area is used.

a) The first is the horsepower² requirement. Since horsepower is directly related to total slot area, additional slots would demand greater horsepower unless the area were proportionately decreased. This decrease cannot, of course, be carried beyond the limits of the milling cutter in producing accurate thin tapered slots.

b) The second limiting imposition is the format-change requirement. Since the tapered section of the bearing creates an asymmetrical cross-section, format changing to accommodate different widths of film would, of necessity, be made from the inside. If more widths were to be handled than could physically be masked between adjacent slots, the bearing would be inoperative.

In view of the foregoing, it is felt that three slots can be used up to and including a 3-inch outside diameter with one additional slot provided for each 1/2-inch above 3 inches. These should be symmetrically located in the top half of the liquid bearing.

² For example, if a bearing supports a 7-pound load on a 0.016-inch cushion at an input flow rate of 10 gpm and a pressure of 0.4 psi, the horsepower can be expressed as follows:

$$\begin{aligned}
 \text{HP}_{\text{input}} &= 10 \left[\frac{\text{gpm}}{\text{ft}^3/\text{min}} \right] \times \frac{1}{7.48} \left[\frac{\text{ft}^3/\text{min}}{\text{ft}^3(\text{lb})/(\text{min})\text{in}^2} \right] \times 0.4 \left[\frac{\text{ft}^3(\text{lb})/(\text{min})\text{in}^2}{\text{ft}\text{-lb}/\text{min}} \right] \times \frac{1}{33,000} \left[\frac{\text{ft}\text{-lb}/\text{min}}{\text{hp}} \right] \\
 &= 0.00233
 \end{aligned}$$

4) Select construction material. Figure 2-3 shows smooth plastic pipe to have superior low-frictional characteristics to other materials tested. There is some advantage in using a transparent material since the effectivity of cleaning can be determined visually. Methacrylate, on the other hand, proved to distort so easily that slot size was difficult to maintain. Certain of the polystyrenes or polypropylenes³ might prove more satisfactory but comparative tests have not been made. High temperature polyvinyl chloride or vinylidene chloride should be appraised since both are completely resistant to photographic chemicals and are more stable than the other materials.

5) Design concentric tube stabilizer. Calculate the inside cross-sectional area of the bearing. Select a tube whose inside area closely approximates the annular area between it and the main bearing housing. Count its wall thickness as dead area, of course. Its length should be one diameter (inside diameter of the main bearing housing) more than the slot width.

6) Determine details of construction. The upstream and downstream plenums (i.e. on either side of the slots) in the bearing should each exceed the slot width by three diameters to minimize the effects of turbulence. All internal and external protuberances should be carefully streamlined and polished to minimize frictional losses and provide smooth flow characteristics. The bearing is so sensitive to obstructions that .003-inch tape used in one experiment to mask the slots was found to adversely affect the film behavior. The amount of taper over the length of the slot is dependent, in the final analysis, on the bearing wall thickness and strength of the material employed. In the experimental bearing tested, 0.021-inches taper per inch was found to be satisfactory but a higher ratio would improve the centering characteristics.

³ Acetic acid, in some concentrations, will attack polypropylene.

No work was performed on format-changing masks. This would have to be tested empirically, bearing in mind that each irregularity introduced by the sleeve would be reflected in performance. The small tilt on the two lower slots, Figure 2-22, overcomes the Bernoulli effect and imparts a slight rotary motion to the film.

The six foregoing steps outline the main considerations in designing this type of end-feed, tapered-slot, self-centering liquid bearing.

BIBLIOGRAPHY

Walker, W. H., Lewis, W. K., McAdams, W. H., and Gilliland, E. R., "Principles of Chemical Engineering," p. 78, Fig. 27, 3rd Ed., McGraw-Hill Book Co., Inc., (1937).

Drew and Genereaux, "Quart, Trans. American Institute Chemical Engineering," 32, 17 (1936).

Lange, N. A., "Handbook of Chemistry," 8th Ed., Handbook Publishers, Inc., (1952).

Hodgman, C. D., "Handbook of Chemistry and Physics," 36th Ed., Chemical Rubber Publishing Co., (1955).

Marks, L. S., "Mechanical Engineers' Handbook," 5th Ed., McGraw-Hill Book Co., Inc., (1951).

Binder, R. C., "Fluid Mechanics," 2nd Ed., Prentice-Hall, Inc., (1950).

Wislicenus, G. F., "Fluid Mechanics of Turbomachinery," 1st Ed., McGraw-Hill Book Co., Inc., (1947).

Dodge, R. A., and Thompson, M. J., "Fluid Mechanics," 1st Ed., McGraw-Hill Book Co., Inc., (1937).

"Standards of the Hydraulic Institute," Page B (VIII)-13, Revised November, 1958.

APPENDIX A
EQUIPMENT AND INSTRUMENTATION

25X1A The liquid bearing test rack (Figure 2-1) consisted of a 147.2 gallon stainless-steel hold tank with a rounded bottom and support skirt, obtained on loan from [redacted]. Its overall depth at the center was 39 inches and 37 inches at the edge. Its inside diameter was 33-3/4 inches. A wooden framework mounted over the tank supported the test bearings.

The liquid flow was provided by a 1-horsepower Corcoran pump, Serial No. 4322, Brg. Nash 1 and 2, rated at 36 gpm against a 45-foot head. The motor was a three-phase, 220-volt, 3.2-ampere, Type PF model rated at 3450 rpm, manufactured by the Doerr Electric Corporation. The pump inlet pipe was Kraloy/Chemtrol 1-1/2 inch IPS, schedule 80, PVC 2210, rated at 235 psi working pressure and 73.4°F temperature. It was provided with a removable plug for priming. At the discharge end, downstream from the flowmeter, the pipe was reduced to 1-inch IPS, schedule 80, PVC II, CS207-60, rated at 327 psi working pressure and 77°F temperature. Flow control was provided by a 1-inch Chemtrol ball valve, Type KC 101. All plastic fittings were manufactured by Tube Turn Plastics, Inc. The inlet to the test bearings was a short length of rubber hose with two standard adjustable stainless-steel hose clamps.

The flowmeter was a [redacted] instrument designed to measure gpm flow of liquids with a specific gravity of 1 (See Table 2-1 and Calibration Chart, Figure 2-2). The flowmeter serial number was D-7526 and its range was 5 to 55 gpm. Using the same data, the Reynolds numbers were calculated and graphed against friction factors (both are dimensionless) for PVC pipe (Figure 2-3). The data for various commercial pipes and tubes was obtained from the literature (Walker, Lewis, McAdams and Gilliland). It is interesting to note how much less the coefficients of friction are for plastic than glass, supposedly the epitome of smoothness.

STAT

The pressure measurements were made on a [redacted] Model 19061 "Supergauge". Its range was 30 inches of mercury vacuum to 30 psi pressure; its movement, connection, and bourdon tube were made of Type 316 stainless steel; its gearing was nylon. It was calibrated and

STAT

STAT

certified by the [redacted] on 7
October 1964. All Centigrade temperatures were measured on a [redacted]
[redacted] "Permafused", etched-stem Centigrade thermometer.
It was a 381mm long, gas-filled mercury type, ASTM 63C precision, No.
4173820, with a range of -8° to $+32^{\circ}\text{C}$. It read to 0.1°C with interpo-
lation to 0.01°C . Fahrenheit readings were taken with a [redacted]
[redacted] (56F) Bomb Calorimeter thermometer. It was a total im-
mersion type No. 1362105, with a range of 66° to 95°F . It read to
 $1/20^{\circ}\text{F}$ with interpolation to 0.01°F .

STAT

STAT

STAT

Two other specialized instruments were built to record data for the research program. The first was a sensitive inclined mercury manometer. It was constructed of accurate-bore Pyrex tubing, 122 centimeters long and 7mm in diameter. Its maximum reading was 40 inches scale, which reduced to 20 inches actual because of its 2:1 slope ratio. This was equivalent to 9.82 psi gage. It could be read to 1/100th of an inch and had an accuracy of 0.2 percent full scale when temperature-compensated. Each leg was provided with a glass tee and pinch clamps for bleeding the lines of entrapped air and for filling the instrument with water. The final readings for the modified tapered-slot bearing were made using a similar inclined manometer with a 4.123:1 slope ratio. The sensing pitot probe was constructed of a modified assayer's blow-pipe.

The second device consisted of a vernier depth gage mounted on a 12-inch steel rule, graduated in 1/100ths of an inch (Figure 2-4). This device enabled a complete traverse to be made over the width of the film to determine cushion depths at different pressures and flows.

APPENDIX B

PRESSURE GRADIENT CHARACTERISTICS

To achieve automatic film centering, it is necessary that the pressure gradient of the fluid bearing be shaped so as to create a balanced condition when the film is centered and a restoring force proportional to displacement when the film is offset in either direction from the center position. A hyperbolic gradient such as that shown in Figure B-1 would provide this effect if the length "L" of the fluid bearing is great enough to accommodate all predictable offsets.

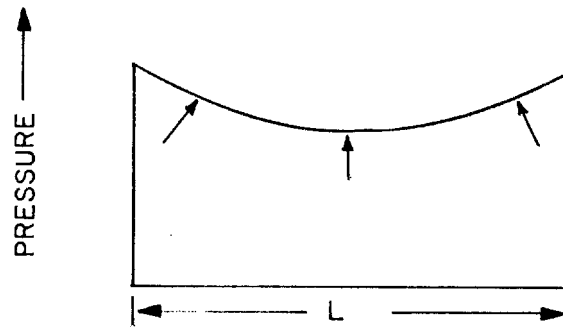


Figure B-1

The abrupt transition from the hyperbolic characteristics to a zero-pressure area at either end of the length "L" is both impossible to realize in an open physical system and unnecessary in a practical sense. A composite characteristic such as that shown in Figure B-2 can be realized and will provide the necessary restoring force. The gradient characteristic should be considered as a composite of three segments, (designated "A", "B", and "C" in the figure. Section "A" represents an approximately hyperbolic characteristic, and is the area of interest. The length " L_1 " of section "A" should accommodate the predictable offsets as described above. Sections "B" and "C" are transition regions that will contribute negative restoring force components if the film excursion extends beyond the useful region. " L_1 ", therefore, must include a safety margin to avoid such occurrence.

APPENDIX B (Continued)

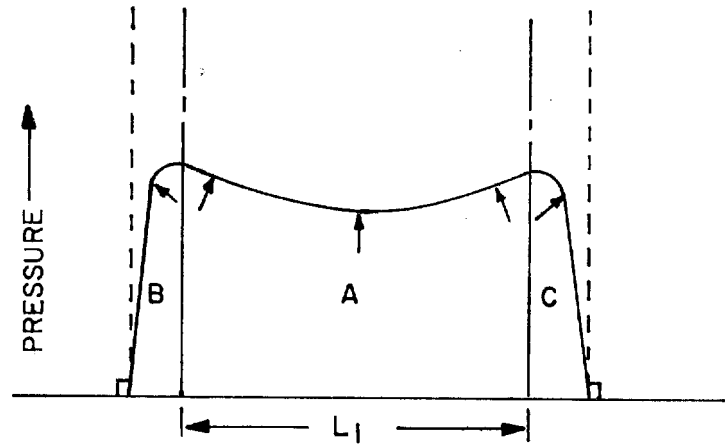


Figure B-2

The specific pressure gradient required for the hyperbolic portion of the gradient characteristic will be influenced by the horizontal and vertical loading forces on the film. These forces are largely a function of the film tension and speed of movement over the fluid bearing.

STATINTL

